ANALYSIS OF WEAR ON AIRCRAFT BRAKE AND LIFE DEVELOPMENT OF ITS FRICTION PADS

Major project report submitted in partial fulfillment of the degree of

MASTER OF ENGINEERING
IN
PRODUCTION ENGINEERING

BY
RAJIB LOCHAN PANIGRAHY
(Roll no: - 12/PE/01)

Under the supervision of

Sh. R.C. Singh

MECHINICAL ENGINEERING DEPARTMENT

DELHI COLLEGE OF ENGINEERING, DELHI.
JULY 2005

DELHI COLLEGE OF ENGINEERING,DELHI

CERTIFICATE

This is to certify that the dissertation entitled **ANALYSIS OF WEAR ON AIR CRAFT BRAKE AND LIFE DEVELOPMENT OF ITS FRICTION PADS** and submitted by **RAJIB LOCHAN PANIGRHY** Roll No. **12/PE/2001** in partial fulfillment of the requirement for the award of the Masters of Engineering In Mechanical Engineering with the specialization in **PRODUCTION ENGINEERING,** is an authentic record of his own work carried out under my supervision. This is further certified that the matter embodied in this dissertation has not submitted elsewhere for the award of any other degree or diploma.

R. C. SINGH
Lecturer,
Mechanical Engineering Department,
Delhi College of Engineering, Delhi.

Place:

Date:

ACKNOWLDGEMENT

I feel delighted to express a few words of gratitude and response to all those distinguished personalities who guided and inspired me in completion of this thesis work.

I am deeply indebted to Mr. R C SINGH, lecturer, Mechanical Engg. Department, Delhi college of Engineering, Delhi for giving me this opportunity to do this thesis work under his continuous guidance and encouragement throughout the thesis without which this work would not have seen light of the day.

I express my sincere gratitude to Dr. R K PANDEY, Asst. Professor IIT, Delhi for his valuable guidance and extending all possible help and all the required facilities to complete my thesis.

I express my gratitude to Prof. C.K DUTTA, Prof. S Maji and Prof. S.K GARG for their hospitality, continuous guidance and encouragement through out the work.

I express my special thanks to Mr. A K BATRA, General Manager (Engineering), Northern region, Indian Airlines, Delhi, and Mr. S K MISHRA Dy General Manager (Engineering) IAL, Delhi for allowing me to complete my masters degree and providing all required facilities whenever required.

My sincere thanks to Mr. Tek Chand, Technician, Mechanical Engineering Department, DCE, Delhi for extending all possible help for preparing samples for the project.

I express my sincere thanks to my friends for giving me suggestions and sharing their experiences with me during the course of my work. I would like to thank all those who helped me directly or indirectly in the completion of this thesis work.

Date: -

RAJIB LOCHAN PANIGRAHY

LIST OF SYMBOLS.

R_a = Arithmetic mean of the departures of the profile from the mean line
R_q = Root mean square of the ordinates
R_p = Maximum height of the profile above the mean line within the sampling length
R_v = Maximum depth of the profile below the mean line within the sampling length
R_s = Skewness is measure of symmetry of the amplitude distribution curve about the mean line
R_{ku} = Kurtosis is a measure of shape (sharpness) of the amplitude distribution
R_z = Sum of the largest peak and the largest valley of the profile within the sampling length
E = Average value.
Z(x) = Height of the profile at a given coordinate along the mean line Z(x)=0.
Z(x+l)= Height of an adjacent coordinate (x+l) taken at an interval from the previous one.
L = Profile length.
σ = Standard deviation of the profile.
$\Psi(z)$ = Probability density function of the distribution of the heights.
Z = Height of the profile measured from the centerline.
W = Specific wear rate.
V = Wear volume.
H = Surface hardness.
w = wear rate.
S = Sliding distance.

ABSTRACT

The sliding of a cerametalic brake pad of an aircraft against a steel rotor under high speed and temperature is different from most tribological system, when worn against the rotor, the complex structure and very inhomogeneous composition of pads results in a particular surface structure, with large contact plateaus rising a few micrometers above the rest surface. When the brake friction pads slide against the rotor, hard ceramic particles embedded between the plates, causes heavy scratches on the friction pads, as in the case of third body abrasion which results in more wear rate of the friction pads.

The present study is to modify the surface profile of the friction pads with making radial equidistance slots, so that better cooling between the rotor and friction pads is obtained and wear loss due to the third body abrasion id minimized. The present study involves a more compressive study of the formation, mechanical properties of the tribological surfaces of aircraft brake friction pads using high resolution scanning electron microscopy. It was observed that the friction pads with four radial slots have better wear resistance property than the existing plane friction pads.

CONTENTS

Declaration
Acknowledgement
Abstracts
List of symbols

Chapter-1 Introduction 1
1.1 Propose and scope of this report 3
1.2 Need for proposed dissertation work 3

Chapter-2 Wear 4
Definition 4
2.1 Effects of wear 4
2.2 Types of wear 5
2.3 Some statistical models of friction of solids 9
2.4 Structural and energy theory of friction of solids 9
2.5 Theoretical and experimental prediction of Performance of multidisc aircraft brakes 10

Chapter-3 Wear Theories 11

3.1 Wear Mechanism 12
3.2 Transition in wear rate 13
3.3 Assessment of surface texture 13
3.3.1 Surface parameters 13
3.4 Statistical analysis of surface profiles in vertical plane 15
3.5 Height distribution of surface texture 15
3.5.1 Skewness 16
3.5.2 Kurtosis 16
3.6 Autocorrelation function of surface profiles 16
3.7 The effect of microstructure on wear models of ceramics 17
3.8 Wear of ceramics 17

Chapter-4 Literature Survey 19

Chapter-5 Aircraft Landing Gear 26

5.1 Landing gear brake 30
5.1.1 Data 30

5.1.2 Description 30
5.1.3 Operation 34

Chapter-6 Experimental work and procedure 35

6.1 Collection of data 35
6.2 Analysis of data 35
6.3 Study of brake lining materials of Boeing 737-200 Aircraft by minor geometrical changes in design of Pads for better cooling 37
6.4 Collection and preparation of the materials for the Experimental work 39
6.5 Test Rig 41
6.6 Sliders 43
6.7 Disks 44
6.8 Test conditions 45
6.9 Discussion 48

Chapter-7 Conclusion 66

References 70

List of figures 71

CHAPTER 1

INTRODUCTION

Since the beginning, men have always felt the need for its equipment and design to optimize its technology. Hence modifications are issued every now then, while collecting all possible data's from the experts, service experience, field survey and experimental results.

The purpose of friction brake is to decelerate a vehicle by transferring the kinetic energy of the vehicle to heat energy via frication and, dissipating that heat energy to surrounding. As a part of an aircraft, the brake materials have additional requirements, like resistance to corrosion, light weight, long life, low noise, stable frication, and low wear rate and acceptable cost verses performance. There are two types of friction brakes i.e. drum/ shoe brakes and disk/Pad brakes. The design of brakes affects heat flow, reliability, noise characteristics and ease of maintenance.

History records the use of many kind materials for brakes (friction materials) for example wagon brakes used wood and leather. Intact many current brake materials still content organic based materials, like Polymer and plant fibers. Emerging railroad technology in the 1800's required brake materials to perform under high load and speed. Frication experiments were conducted with iron brake shoes in 1870's.

In order to achieve the properties required of brakes most brake materials are not composed of single elements or compounds but rather are composites of many

materials. More than 2000 different brake materials and their variants are now used in commercial brake components (Weintraub 1998).

According to Nicholson (1995). Herbert Frood is credited with inventing the first brake lining materials in 1897. It was a cotton-based material impregnated with bitumen solution and was used for wagon wheels as early automobiles. His invention lead to the founding of the Ferodo Company, a firm that still supplies brake materials today. The first brake lining materials were woven, but in the 1920's these were replaced with molded materials that contains crysotile asbestos fibers, a plentiful mineral. Resin- bonded metallic linings were introduced in the 1950's and by the 1960's so called semimetals were developed. These contain a higher amount of metal additives.

The history of brake material shows that some of the simplest compositions (fiber plus resin) can be effective, but here have been all kinds of commercial additives introduced and promoted. The ratio of resin to carbon to metallic fibers in semi-metallic brake materials has changed very little during the 20^{th} centaury. On the other hand there are 6 types resins alone. The reasons for so many additives are partly based on function but also on ingredient cost, availability and processing issues. Nicholson (1995) reports that the same ingredients can be sent to several plants and resulting brake can have friction coefficient that vary by a factor of two. Therefore frication brake composition is only a part of picture in ensuring satisfactory brake performances.

Aircraft brakes primarily consist of resin/ steel metallic lining and carbon-carbon combinations. The C.C. Combinations are more commonly used in high performance brakes due to their high temperature characteristic. The ability of the

material is to stand up under rejected take-off (RTO) condition is another important requirement. The friction coefficient for C.C. varies significantly with interface temperature. Therefore braking performance varies under low hand high-energy conditions.

1.1. PURPOSE AND SCOPE OF THIS REPORT

The purpose of this report is to present survey of aircraft brakes to indicate their typical properties and functions. Brake materials test methods are also briefly described. This report does not address issues associated with materials and additives of brake materials. Since there are literally thousands of brake material additives and their combinations are nearly limitless and also non-availability of composition of the specimen it is impracticable to study on the constituents and their function. Rather an attempt has been made to focus on design of the friction pads.

1.2. NEED FOR PROPOSED DISSERTATION WORK

The aircraft landing system main gear brake assembly for Boeing 737-200 twinjet short haul transport airplane is designed and manufactured to the highest quality standards, to provide the user optimum service life at a minimum cost. However a survey on ten brake units for ten full worn out condition removals revealed that some brake units stand up to brake application of 1461 aircraft landings, while others last for only 332 aircraft landing brake applications. Due to very high range of collected data, an attempt is made to increase life of the brake friction pads for high-energy stops. Since the aircraft part replacement labour costs very high, an increase in life of the brake friction pads will save a lot for the airlines and the economy of the country.

CHAPTER -2

WEAR

Definition

Wear is the progressive damage, which occurs on the surface of a component as a result of its motion, relative to the adjacent working parts. It is defined as removal of material from the surface of component . It depends on many variables such as

(i) Hardness

(ii) Impact strength

(iii) Toughness

(iv) Modulus of elasticity

(v) Corrosion resistance

(vi) Fatigue resistance

The other factors like**: -**

(i)Surface finish

(ii) Lubrication

(iii) Load

(iv) Speed

(v) Temperature

(vi) Properties of opposing surface etc.

2.1 The effects of wear are

(i) The cost of replacement of parts

(ii) The expenses involved in machine down time

(iii) Lost production and consequent loss of business opportunities

(iv) The decreased efficiency of worn plant equipment resulting in inferior performance and increased energy consumption.

There are many types of abnormal wear that can exist inside a piece of machinery. Although there are many different types of wear, there are only a few primary sources of the wear. Problems related to the oil itself may contribute to wear, in cases where the lubricant has degraded or become contaminated. The machine condition can also contribute to the generation of wear, if a component is misaligned or improperly balanced. Improper use of the equipment such as overload or accelerated heating conditions can also generate wear.

2.2 TYPES OF WEAR:

Below are some examples of the different types of wear that can occur.

- **Abrasive Wear** is the results of hard particles coming in contact with internal components. Such particles include dirt and a variety of wear metals. Introducing a filtration process can reduce abrasive wear. It is also important to ensure vents, breathers, and seals are working properly. The harder asperities trapped at the interface, when moving relative to the surface, cause abrasion of the surface and the resulting damage is called abrasive wear. The abrasive wear mechanism is basically same as machining, grinding, polishing or lapping that are used for shaping materials. The body abrasive wear occurs when one surface (usually harder than the second) although this mechanism very often changes to three body abrasion as wear debris then acts as an abrasive between two surfaces.

Abrasive can act as in grinding where the abrasive is fixed relative to one surface of as in lapping where the abrasive tumble producing a series of indentations as opposed to scratch.

Archard has proposed an equation

$$V/L=K_{ab}\ W/H$$

In this equation K_{ab} represents the non-dimensional abrasive wear coefficient. The coefficient depends on the nature of the abrasive and extent of cutting action.

One important parameter is the relative hardness of the abrasive to that of the metal. When this ratio exceeds 1.4 strong abrasive action is expected. In general the adhesive wear coefficient tend to be higher for metallic material in comparison to adhesive wear. It is hence important to have efficient filtration system to remove abrasive contaminants.

- **Adhesive Wear** is when two metal surfaces come in contact allowing particles to break away from the components. Insufficient lubrication or lubricant contamination normally causes this. Ensuring the proper viscosity grade lubricant is used can reduce adhesive wear. Reducing contamination in the oil will also help eliminate adhesive wear. Adhesive wear is produced by the formation and subsequent shearing of welded junction between two sliding surfaces. For adhesive wear it is necessary for the surfaces to be in intimate contact with each other. Surfaces, which are held apart by lubricating films, oxide films etc. reduce the tendency for adhesion to occur.

  Archard' equation for adhesive wear is

  $$V/L= K\ W/H$$

  Where V = Wear volume

  L = Sliding length

W = Normal load

H = Hardness

K = Wear coefficient.

- **Cavitations occur** when entrained air or gas bubbles collapse. When the collapse occurs against the surface of internal components, cracks and pits can be formed. Normally cavitations originates from changes in pressure in the liquid brought about by turbulent flow or by vibration, but can also occurs when bubbles or cavities collapse on or very near the eroded surface. The mechanical shock induced by cavitations is similar to that of liquid impingement erosion causing direst localized damage of the surface by inducing fatigue. Controlling foaming characteristics of oil with an anti-foam additive can help reduce cavitations.
- **Erosive wear** is caused by a gas or liquid, which may or may not carry entrained solid particles, impinging on a surface. When the angle of impingement is small, the wear produced is closely analogous to abrasive. When the angle of impingement is normal to the surface, material is displaced by plastic flow or is dislodged by brittle failure.

- **Corrosive Wear** is caused by a chemical reaction that actually removes material from a component surface. Corrosion can be a direct result of acidic oxidation. A random electrical current can also cause corrosion. Electrical current corrosion results in welding and pitting of the wear surface. The presence of water or combustion products can promote corrosive wear.

- **Cutting Wear** can be caused when an abrasive particle has imbedded itself in a soft surface. Equipment imbalance or misalignment can contribute to

cutting wear. Proper filtration and equipment maintenance is imperative to reducing cutting wear.

- **Fatigue Wear** results when cracks develop in the component surface allowing the generation and removal of particles. Fatigue wear can occur in non-conforming machine elements such as rolling element bearing and gas in the form of rolling contact fatigue and pitting. It occurs when the contact stresses approaches the elastic limit. The number of stress cycles necessary to cause failure decreases with increasing stress. Leading causes of fatigue wear include insufficient lubrication, lubricant contamination, and component fatigue.
- **Fretting wear** is a small amplitude oscillatory motion, usually between two solid surfaces in contact. Fretting wear occurs when repeated loading and unloading causes cyclic stresses, which induces surface or subsurface break-up and loss of material. Vibration is a common cause of fretting wear.

- **Sliding Wear** is caused by equipment stress. Subjecting equipment to excessive speeds or loads can result in sliding wear. The excess heat in an overload situation weakens the lubricant and can result in metal-to-metal contact. When a moving part comes in contact with a stationary part sliding wear becomes an issue.
- **Delamination wear** is a form of wear in which loss of material is in the form of thin flaked or platelets. This type of wear is caused by the surface traction exerted by the harder asperities induces plastic shear deformation of the softer surface which accumulates with repeated loading. As the surface deformation continues, cracks are formed below the surface in the vicinity of preexisting defects (voids and inclusive). Once cracks are present further

loading and deformation causes this to propagate parallel to the surface and this generally give rise to delamination resulting in thin wear sheets. .

2.3 Some statistical models of frictional contact.

Contact is discussed of real surfaces with a broad scale range of asperities. Results of simulation are presented of rough contact with adhesion. Real contact area is shown to be governed by adhesion parameter, which is characterized by a relation of surface force and pull-off force of surfaces in contact.

2.4 Structural and energy theory of friction of solids.

A thermodynamic system is considered comprising two bodies in frictional contact. In the cycle involving formation of the contact, its movement over the crystallite and disruption after intersecting the boundary of the crystallite variations of the potential is demonstrated to be $\Delta G = 0$. Once the contact has been formed, system's surface reduces by the doubled actual contact area. This is accompanied by heat dissipation: $-\Delta G = \Delta \Omega E = 2A_r E = \delta q$, whereas $\Delta G = 0$ when the contact moves over the crystallite. Disruption of the contact results in a rise of the thermodynamic potential, for which purpose a work $A = \Delta G = 2A_r E$ should be expended. Therefore, the specific adhesion is $\tau_0 = 2E/L$. The share of work done by the friction force to produce debris is $\beta = 6nIE/PL$. Within the measurement error, the experimental and calculated friction parameters are in agreement for some metals, carbon-based materials and polyethylene.

2.5 Theoretical and experimental prediction of performance of multiple-disc aircraft brakes

Different combinations of materials are used in multiple-disc aircraft brakes. Stability and fluctuations of braking torque (friction coefficient) should be at the specified level, the braking is consistent and efficient, and the brake efficiency should be as high as possible to provide gradual braking and maximum wear life. Test-calculation method is proposed to assess the friction pair at the stage of design. The method is based on the theory of thermal dynamics and simulation of contact at dry friction and boundary lubrication. Particular attention is paid to the influence of the number and design of slots on rotating and stationary discs and their optimal amount in the pack.

CHAPTER-3

WEAR THEORIES

Wear depends on many variables, wear research programme must be planned systematically. The wear maps recently proposed by Lin and Ashby use normalized stresses and velocities to draw together much published data on the wear of steel. To the extend that these maps reveal clear patterns of wear rates, they may be very useful. Wear maps of the type already published, or of some different type yet to be developed.

The familiar wear coefficient ‘k’ represents another way of normalizing wear data In this case ‘k’ is generally assumed to be the proportionality constant in simple linear wear law of the form V=kLS\H, where V is the wear volume, L is the normal load, S is the sliding distance and H is the hardness of the wearing material. Such an equation has been proposed by many investigators. It can be derived by using models based on abrasion, adhesion, fatigue, oxidation etc. In each case the equation is based on a simplified model having a limited number of variables. The coefficient ‘k’ is assumed to be constant. So it should be used with caution if an application requires extrapolation outside the range of available experimental. Dramatic transitions in wear rate are well known. There fore, if a linear wear law is used, it should not be surprising to find that ‘k’ dose not remain constant.

The coefficient k has been interpreted in various ways. These include the probability that an asperity contact event generates a wear particle, the fraction of asperities, which yield debris particles, the ratio of the volume worn to the volume plastically deformed, and as a factor inversely proportional to the number of loading cycles needed to produce a wear particle. All of these are connected to the small size of k, i.e. each involves a different physical reason why wear is an inefficient process.

That so many different physical can lead to the same form for a wear equation could be thought of as strong support for using this equation. However, it is tempting to think in terms of particular model when using the linear wear equation, and this can bias a user in a particular direction. There is an alternative way to normalize wear data which is closely related but has the advantages of being less tied to specific models. This is the specific wear rate, or V\LS. It is

simply based on the frequent observations that wear is often - not always- proportional to normal load and to sliding distance. The specific wear rate is readily determined from easily measures quantities, and it is relatively free of bias connected with favorite wear theories.

Abrasion is one form of wear, which is relatively efficient if a significant portion of contact events is of cutting-type [15]. It is convenient to think of a given wear situation as being part of a spectrum with cutting at the left side and less efficient wear mechanisms towards the right. With that picture, abrasion processes are intermediate, with the most efficient ones towards the left an others further right. Cutting requires indentation, which depends on hardness, so it is not surprising that abrasion theories and technology acknowledge the importance hardness, at least for ductile materials. For brittle materials there is good evidence that fracture toughness can be more important. For sliding wear process, which are at the right side of our spectrum, the role hardness is more complicated. It certainly effects plastic deformation of near surface material, but other factors are also important, and they make hardness less useful as a guideline for estimating sliding wear resistance compared with abrasion resistance. This would support increased use of specific wear resistance, which does not include hardness, in place of wear coefficient

3.1 WEAR MECHANISM.

The wear rate of a sliding or rolling contact is conventually is defined as the volume of material lost from the wearing surface per sliding distance (U/L, denoted by w) in units of (Light) 2. For a dry and unlubricated sliding contact the wear rate depends on (i) initial temperature, (ii) thermal, mechanical and chemical properties of materials in contact.

There are many physical mechanisms that contribute to wear and no simple and universal model is applicable to all situations. Wear can be caused by adhesion, abrasion, oxidation, delamination and corrosion as well as by variety of other phenomena such as fretting, cavitations and erosion. A common starting point in investigation of the quantitative aspects of wear is the Archrd’s wear equation which states that wear is inversely proportional to the surface hardness H of the wearing material, i.e.

$$W = V/L = K.W/H$$

The dimensional coefficient ‘k’ is known as the wear coefficient. In practical situation, the hardness of the uppermost layer of the material in contact may not be

known with certainly because it becomes a work-hardened surface during repeated sliding. The ratio K/H is known as the dimensional wear coefficient in units of $mm^3\ N^{-1}.m^{-1}$. It represents the wear volume per unit sliding distance per unit load.

Wear may be classified as mild of severe wear. For any pair of materials, increasing the severity of operation by increasing either the normal load, sliding speed or bulk temperature leads at some stage to a comparatively sudden jump in wear rate. The differences in mild and severe wear are:

	Mild wear	**severe wear**
1.	Surfaces-often better than the original	Surfaces, much rougher than the original.
2.	Wear debris extremely small, typically only 100 nm diameter particles.	Large metallic wear debris, typically up to 10 micrometer diameter
3.	High electrical contact resistance, little true metallic contact.	Low contact resistance, new metallic junction formed.

3.2 Transition in wear rate

The wear rate of a pin of leaded brass against a hard stelite ring as a function of normal load. At low loads, the wear rate increases with load. At loads between 5 and 10 N There is a sharp increase in wear rate by a factor of about 100. Beyond this the wear coefficient is about 10^{-4}

3.3 ASSESSMENT OF SURFACE TEXTURE

The quantitative assessment (distributions, sizes and shapes of the asperities) of the topographic features of surfaces is of great importance in tribology. A typical surface might have million of hills and valleys. Measuring the height and location of each peak would be formidable. There fore irregularities measurements are generally done on small but representative sample length varies from 0.8mm to 25mm. The upper limit is commonly accepted for most waviness surfaces.

3.3.1 Surface parameters

The stylus method reveals only a single plane property of the surface topography and its characterization has to be based on the nature of the ensuing single line profile. In manufacturing engineering one of the two parameters is usually based to define the surface texture. These parameters are CLA (center-line average, Ra) roughness value, and the RMS (root mean square, Rq) value. The

CLA is defined as the arithmetic average value of the vertical deviation of the profile from the centerline, and the RMS value as the square root of the arithmetic mean of the square of this deviation.

In mathematical form these can be written as:

$$Ra = \frac{1}{L} \int_0^L I\, Z\, I \, dx$$

Where
z = height of the surface measured above the mean level i.e. the line drawn such that the area of hills above is equal to that of the valleys below.
x = coordinate in the surface.
L = sample length (this length is often set to be five times of longest wave length of profile fluctuations)

One difficulty in using Ra value is that they may fail to distinguish between a relatively gently undulating surface and one with a much spikier profile. Both surfaces exhibit significantly different tribological properties. The RMS roughness parameter Rq goes some way to overcome this difficulty, from its definition the square term gives greater significance to surface variations some way from mean.
These parameters (Ra and Rq) are seen to be primarily concerned with the relative departure of the profile in the vertical direction only. They do not provide any information about the slopes, shapes and sizes of asperities or about the frequency and regularity of their occurrences. It is possible, therefore, for surfaces of widely differing profiles to give the same CLA or RMS values. Abbott and Firestone the founders of profilometry, were concerned with the wear behaviour of surfaces, and they choose their parameters accordingly in their studies. Using the profile of a surface they constructed its bearing area curve by measuring the fraction of the sample length which lies inside the profile at various positions above the lowest point on the profile as shown in the figure. By dividing the surface into three height zones, containing the highest 25%,middle 50%and lowest 25%of the bearing area curve, they identified three parameters- the peak, medial and valley occurrences respectively.

3.4. Statistical Analysis of Surface Profiles in the Vertical Plane

The micro-texture of the surface of a component used in engineering is irregular and for its description the following stastical parameters are essential.

3.5. Height Distribution of Surface Textures

The texture of a surface can be described in terms of the distribution function of its profile heights. In statistical terms the cumulative distribution of the all-ordinate distribution curve is

$$F(z) = \int_{-\infty}^{\infty} \psi(z)\, dz$$

where
z = height of the profile measured from center line
$\psi(z)$ = Probability density function of the distribution of the heights

The practical deviation of such distribution curves involves taking measurements ofZ1, Z2,…. etc. at some discrete interval's and summing the number of ordinates at any given height level. The distribution curve of this figure is smoothest curve that can be drawn through the histogram produced by such a sampling procedure. The smooth curve for many surfaces tends to exhibit a Gaussian distribution of surface texture heights.

The curve of the Gaussian distribution or density function of heights is given by

$$\psi(z) = \psi_0(z) e^{-z^2/2\sigma^2}$$

Where,
σ = Standard deviation of the distribution,
There are engineering surfaces whose textures show certain departures from Gaussian distribution and it is necessary to define some statistical parameters, which may measure these departures.

3.5.1 Skewness

The skewness is a measure of the departure of a distribution curve from symmetry. This is defined as

$$K = \frac{\int_{-x}^{x} z^3 \Psi(z)dz}{\sigma^3}$$

Symmetrical Gaussian distribution curve have zero skewness, unsymmetrical curves can have either negative or positive skewness.

3.5.2. KURTOSIS

The kurtosis is a measure of the hump on a distribution curve. This is defined as

$$K = \frac{\int_{-x}^{x} z^4 \Psi(z)dz}{\sigma^4}$$

Gaussian distribution curve has a kurtosis of 3, which is usually taken as standard value for the kurtosis. Curve with values of k less than 3 are called platykurtic and those with k greater than 3 are called leptokurtic.

3.6. Autocorrelation Function of Surface Profiles

The previously discussed parameter depends only on the profile heights, not on the spacing between heights. As a result they do not truly reflect the shape of the profile. The autocorrelation does incorporate the spacing between heights and is obtained by multiplying each profile by the height of the point at some fixed horizontal distance (l) farther along the profile.
After averaging the product over a representative profile length (L), the auto correlation function is:

$$R(l) = E\,(z(x).\, z(x+l))$$

Where,
E = average value
Z(x) = height of the profile at a given coordinate x along the mean line z(x) =0

Z(x+l) = height at an adjacent coordinate (x+l) taken at an interval'l' from the previous one.

If the value of the ordinates at discrete interval 'l' is known

$$R(l) = \lim_{L-x} \frac{1}{L} \int_{-L/2}^{L/2} z(x) x Z(x+l) dx$$

A typical plot of the autocorrelation function for two different profiles is shown in fig. The shape of this function is most useful in revealing some of the characteristics of the profile. The general decay of the function, R(l), indicates a decrease of correlation as 'l' increases and is an indication of the random component of the surface profile, while the oscillatory component of the function indicates inherent periodicity of the profile.

3.7. The effect of microstructure on wear model of ceramics

The effect of the microstructure on the wear modes in structural ceramic materials was studied in two SiC and three AL2O3 materials. IN each class of materials, it was observed that the predominant damage mode is determined by the microstructure of the material. The materials with weak grain boundaries were found to wear primarily by grain pluck out and so showed more wear than did (the one, a-SiC) materials with stronger grain boundaries. In addition, the presence of a softer second phase around the grain boundaries, which in commercial materials is usually more ductile than the grain, changed the mode and amount of damage, resulting in improved wear resistance (only in repeated passes). Under repeat pass sliding, the amount wears increased considerably in all the materials except the material with a softer second phase.

3.8. Wear of ceramics.

There are two types of wear encountered with ceramics. These are adhesive and abrasive. Adhesive wear occurs when adhesion takes place across an interface between two ceramic surfaces or a ceramic surface and a metal. With tangential motion, i.e. the sliding of rubbing of one surface over the other, if fracture occurs in the ceramic, adhesive wear has taken place. For this type of wear exist, adhesion must first occur. Secondly the fractured strength of one of the two materials in contact must be less than that of the interfacial junction. If bonding in the

interfacial junction. If bonding in the interfacial junction is less than that in either of the two materials, fracture will occur at the interface with theoretically no wear occurring.

The presence of surface and subsurface defects such as dislocations, vacancies, voids, impurities and micro cracks in the surfacial layers of the materials in contact will generally dictate the zones from which wear damage and wear particles are generated. The extent and distribution of such defects will, to a large extent, determine the size of the wear damage and wear particles generated. This is observed in scanning electron microscope.

Abrasive wear occurs when two surfaces, one considerably harder than the other, are brought into contact. If a hard particle or hard asperity of approximately spherical shape is in contact with a ceramic under load, the ceramic initially deforms locally according to the well-known heritzian elastic equation. Fractures with ring cracks have been produced in flat surfaced ceramics critically loaded either statically or dynamically with hard spheres.

Abrasive wear can also occur when a third particle harder than one or both of the surface in contact becomes trapped at the interface. It can then operate to remove material from one or both surfaces. This mode of wear is then the so-called three-body abrasion.

CHAPTER-4

LITERATURE SURVEY

Despite the enormous amount of testing and development of automotive brakes and brake pad materials, rather little is known about their tribology contact situation on a microscopic level. The sliding of a ceramic brake pad against a steel rotor is different from most tribology systems. The researchers/authors who are from different industrial backgrounds have their views and experience about wear on brake pads through various technical journals and books. This chapter briefly covers the background research that has been done on wear of brake pads.

S K Rakhee [24] emphasis that the wear of a metal reinforce phenolic resin increases exponentially with increasing temperature. On 1974 he suggested that the wear of metal is controlled by a pyrolysis mechanism at elevated temperatures and by adhesive and abrasive mechanism at low temperature.

H D Bush, D M Rowson and S E Warren [23] discusses the ways to measure wear of friction materials and disc obey a modified form of Archad's wear law over a range of operating temperature

O O Ajayi and K C Ladema [13] discuss the effect of microstructure on wear modes of ceramic materials. They concluded that the materials with weak grain boundaries were found to be wear primarily by grain pluck out and so showed more wear than did materials with stronger grain boundaries. The presence of a softer second phase around the grain boundary is more ductile then the grain, results in more wears resistance. Under repeat pass sliding, the amount of wears increases considerably in all the materials except the material with softer second phase.

Etsuo Marui, Masatoshi Hashimoto, Shinobu Kato and Wataru Kojima [11] on their work on dissipation of kinetic energy by slip at the interface of the mating surfaces suggested that the material damping originated by inelastic and elastic dislocation movements within grains and also slip at grain boundaries in materials. The structural damping, which offers excellent capacity for large energy dissipation, initiating from the interface shear at separable structural joints. The slip and dissipation energy at the interface are influence by the kind of the materials, the surface finish and the clamping conditions.

C S Ramesh, S K Sheshadri and KJL Iyer [12] presented a model for wear rates of polymer-based composites under sliding conditions. Wear resistance increases with the increase in volume percentage of silicon nitride in the nickel matrix.

A Fisher [15] discussed the mechanisms of high temperature sliding abrasion of metallic materials. He suggested that up to 650° C the wear rate decreases with increasing temperature. The fragments of flint particles penetrate into the softer surfaces, in addition layers are generated which adhere strongly to the abraded areas of the specimen. These fragments and layers protect the surface against abrasion.

Takahisa Kato & Hiroshi Soutome [7] conducted friction and wear characteristics of each component of the disc brake Pads were analyised stochastically by multiple regression analysis using database preliminarily prepared by friction and wear test. Genetic algorithms for the given coefficient of friction optimized the composition of the brake Pad. It has a remarkable potential for the design of friction materials.

Yuji Honda and Takahisha Kato [10] suggested the effect of Cu powder, $BaSO_4$ and cashew dust on the wear and friction characteristics of automotive brake pads. The friction and wear characteristics of the slider made of Cu powder $BaSO_4$, cashew dust, phenolic resin and aramid fibers were studied experimentally by using a slider-on-desk type tester. These materials are major components of the brake pad in service. It was found that the sudden decrease in friction co-efficient occurred with increase surface temperature. However when $BaSO_4$ was not included in the slider, the wear rate was remarkably increased. $BaSO_4$ has effects on the increase in strength of the slider and on the decrease in the wear

DA Rigney [14] gave few thoughts on sliding wear. He said wear depends on many variables.

The wear volume $V = KLS/H$

Where K= co-efficient

L = normal load

S= sliding distance

H= hardness of wearing material.

Peter J Blau [5] discussed the composition, functions, and testing of friction brake materials and their additives. The various levels of brake material testing are

1. Vehicle Road tests.
2. Vehicle skid-pad test.
3. Vehicle drive-on Dynamometers.
4. Inertial Dynamometers.
5. Laboratory Tribometers.

G W Stachowiak, G B Stachowiak and A W Batchelor [18] have said that the metallic films on the ceramic surfaces acted as a form of protection against wear, leaving most of the original ceramic surfaces undamaged. The wear and friction behaviour of metal ceramic sliding pairs is influenced by the nature and mechanical properties of the mating metallic materials. Lower values of co-efficient of friction are recorded for soft metal-ceramic pass (e.g. Brass-ceramic) and few metal ceramic combination generate very high coefficient of friction value and noise levels.(e.g. Steel-Sailon and cast iron-sailon)

K H Zum Gahr [16] has emphasized that the ceramics may be more wear resistance than the steels. The wear rate can be enhanced with ceramic-ceramic and reduced with ceramic-steel material. Plastic deformation, brittle fracture and tribochemical process are reported to be the main mechanisms involved in wear of ceramic materials.

A W Ruff [17] has made a comparison study of standard test methods for non-lubricated sliding wear.

A G M Hunter and E A Smith [21] have suggested that the measurement of single roughness constant completely characterizes a rough surface. Estimating the roughness of a surface is usually a process of estimating either the form and magnitude of the variable spectral density function or magnitude of some average such as root mean square amplitude.

Donald H Buckley and Kazuhisa Miyoshi [20] on their study on ‘Friction and wear of ceramics’ concluded that the contact load necessary to initiate fracture in ceramics is reduced with tangential motion. Both friction and wear of ceramics are anisotropy and relate to structure. Grit size effect in two- and three body abrasive wear. Both free energy or oxide formation and the d-valance bond character. Of metals are related to the friction and wear characteristics for metals in contact with ceramics. Surface contaminants effects friction and adhesive wear.

Generally two types of wear encountered with ceramics i.e. adhesive and abrasive.

(i) The catastrophic cracks may grow easily by application of a shearing force during sliding.

(ii) The deformation and fracture behaviour of the ceramic material is very dependent on crystallographic orientation.

Joseph C Conway, Jr and Robert N Pangborn, Paul H Cohen and Donald A Love [19] discussed on dry sliding wear behaviour of AN-Si-O-N ceramic. They concluded that,

(i)The steady wear rate increases with increase in applied contact load over the range of sliding velocity

(ii) The wear rate is approximately inversely proportional to sliding velocity at the highest contact load level (1600N). For the lowest and intermediate contact load levels, the wear rate has inverse effect on low range sliding velocity and no effect at higher range of sliding velocity.

(iii) Brittle fracture appears to be the primary wear mechanism at high contact loads and low sliding velocities. Plastic deformation mechanisms are continually active, however their roll increases with increasing in sliding velocity.

C H Zum Gahr [9] has said that the abrasive wear can be caused by hard particles sliding on a softer solid surface and displacing or detaching materials. Frequently resistance against abrasive wear is only considered as function of hardness of wearing material. However the nature of interaction, the capability of deformation or the fracture toughness of the wearing material is very important in addition to hardness. Abrasive wear can be substantially be improved by second phase embedded in a hard or soft matrix.

Mikail, Eriksson and Staffon Jacobson [8] suggested that the sliding of an organic brake pad against a grey cast iron rotor is very different from the most tribological systems. When worn against the rotor, complex structure and very inhomogeneous composition of the pads, results in a particular surface structure with large contact plateaus raising a few micrometers above the rest of the surfaces. During each braking, even if performed at constant speed and pressure, a friction increase can be observed. The magnitude of this increase varies with pad materials, state of run in and relative humidity. For a rough and irregular topography the coefficient of friction during the first stop will be much lower than during the following. The friction increase will be larger during the first stop and gradually reduces during the following stops.

For some pad materials, the coefficient of friction is considerably higher when braking with decreasing brake pressure than the increasing brake pressure.

The friction increase during run-in of a ground brake pad is primarily co-related to the formation of primary plateaus, as the rough surface of a ground pad is worn, there by increasing the possible area of real contact between the pad and disc. As the area of real contact increases and the surfaces are worn smooth, the element of elastic contact increases and accordingly the area of real contact. An increased area of real contact for a given normal load is believed to result in an increased coefficient of friction. The formation of secondary plateaus at higher brake pressure will relieve the metal fibers carrying the frictional and normal loads. This reduces the risk for seizure between the pad and disc, and also shifts the average composition of the material in frictional contact against the rotors.

Taylor Hobson [6] in his book 'Exploring Surface Texture' Describes the background information on the surface texture and the stylus type measuring instruments and gives useful information's on parameter, their derivation and use.

Yeau-Rin-Jing, Zhi-Way Lin and Shiuh-Hwa Shyu [4] Describes the method to measure the wear of general engineering surface based on the roughness parameters of the worn surface. It simplifies the procedure for the determination of wear comparable to surface roughness with such a method. The profilometrical method for wear evaluation will be more accessible.

H F Stott [3] suggests that the temperature can have a considerable effect on the extent of wear damage to metallic components. Suring reciprocating sliding, under conditions where frictional heating has little impact on surface temperatures, there is generally a transition from severe wear to mild wear after a time of sliding that decreases with increase in ambient temperature. This is due to the generation and retention of oxide and partially oxidized metal debris particles on the contacting load bearing surfaces; these are compacted and agglomerated by the sliding action, giving protective layers on such surfaces. At low temperature from 20 to 200^0 C, The layers generally consists of loosely compacted particles; at higher temperatures there is an increase in the rate of generation

and retention of particle while compaction, sintering and oxidation of the particles in the layers are facilitated, leading to development of hard, very protective oxide glaze surface.

A transition from severe wear to mild wear is observed during reciprocating sliding at ambient temperature of 20- 800^0C. This is associated with the establishment of compacted layers of wear debris particles. At the higher temperatures further oxidation, compaction and sintering can lead to development of hard oxide glaze surface layer leading to very low rate of wear. So the increased temperature facilitates the generation of oxide debris and assist in compaction of debris, to develop the wear protection cover.

Noureddine Tayebi, Andreas A Polycarpou [2] state that engineering surfaces possess roughness that exhibit asymmetrical height distributions. They predicted that the surfaces with high kurtosis and positive skewness exhibit lower static friction and friction coefficient. It is predicted that, for high kurtosis values, the static friction coefficient decreases with decreasing external force rather than increasing as seen with increasing skewness. It is found that positive skewness results in lower friction coefficient values, while negative skewness results in higher values than the Gaussian case. The effect of kurtosis on the static friction coefficient can be completely different. While the same effect as the skewness is found for kurtosis ≤ 3, different trends are observed for kurtosis >3. It is found that μdecreases with decreasing external forces rather than increasing sharply as seen with the effect of skewness, and predicting much lower values for static friction coefficient.

R K Pandey and O P Gandhi [1] on their book on ‘Advances in Tribology and Maintenance’ have systematically described the mechanism of wear, Texture of engineering surfaces, mechanism of friction and overview of tribological applications etc. They have stated the procedures for assessment of surface texture and surface parameters.

Maintenance manual of Boeing 737-200 aircraft.

Component reference manual of brake unit of Boeing 737-200 aircraft describes the internal construction of the brake unit.

Training manual of Boeing 737-200 aircraft gives brief idea about the description operation of landing gear and braking system of Boeing 737-200 aircraft.

CHAPTER-5

AIRCRAFT LANDING GEAR.

Landing gear is a vital part of an aircraft. It supports the aircraft on ground and takes whole load of the aircraft during parking, towing, taxying, take-off and landing. It also observes the vertical downward force of the aircraft and horizontal velocity of the aircraft weight during braking.

The landing gear consists of two main landing gears and one nose landing gear. Each main landing gear is located aft of the rear wing spar inboard of the engine nacelle. The nose landing gear is located below the aft bulkhead of the central cabin.

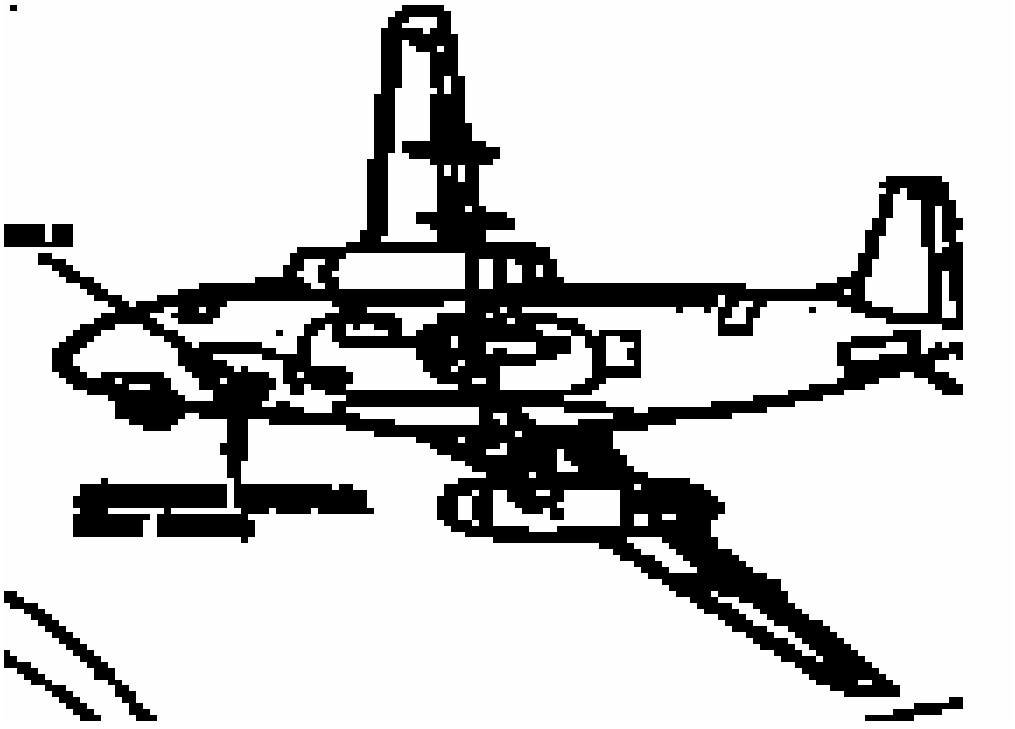

Fig 1. Landing Gear System.

The main landing gears provide aft support for the fuselage. The main and nose landing gear use air-oil type shock strut to observe impact on landing and vibration and shock from movement of the airplane on the ground. Each main landing gear and nose landing gear is equipped with two tyres and wheel assembly. Each main landing gear is fitted with disc type hydraulic brakes modulated by an antiskid system. Each main landing gear also transmits the braking force to the airplane structure.

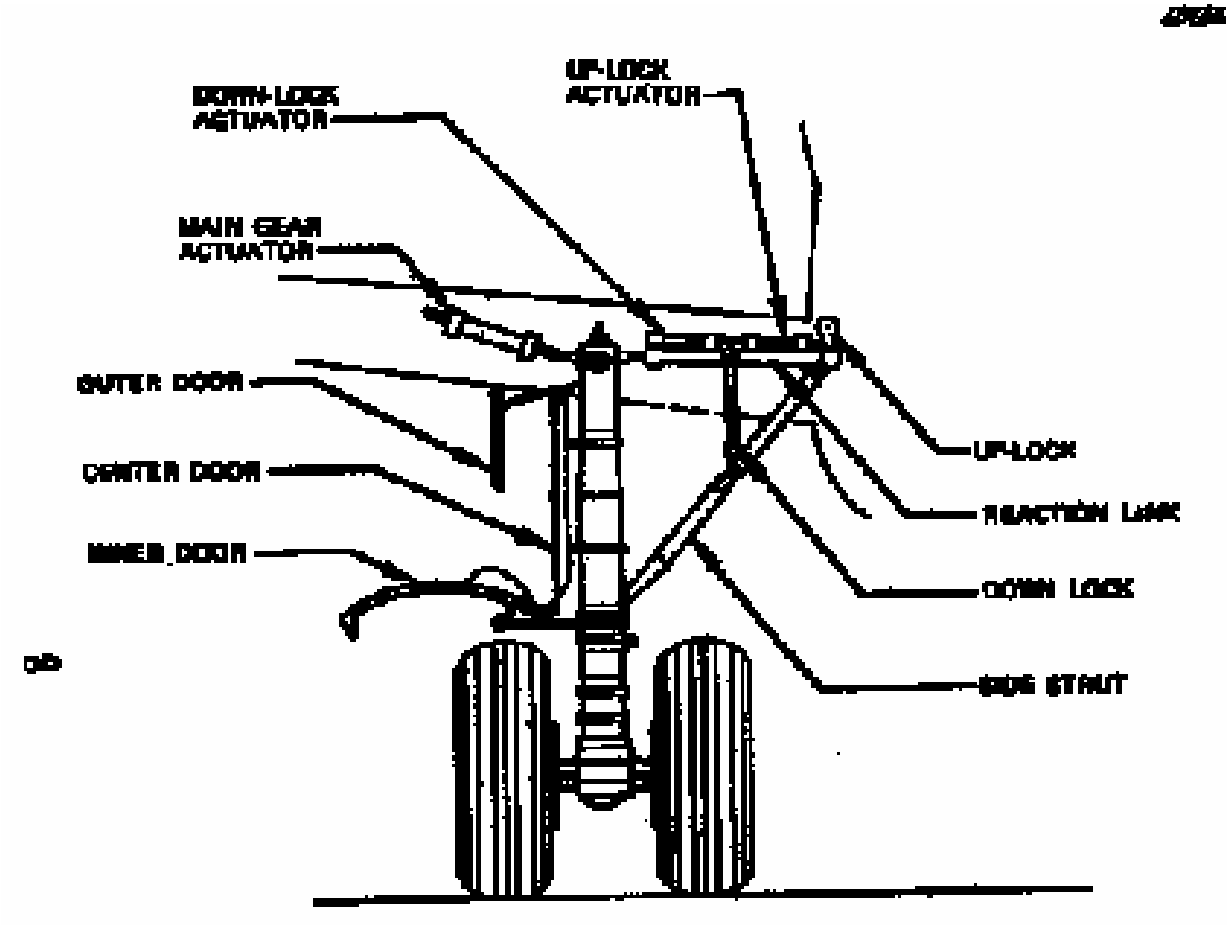

Fig 2. Main Landing Gear

The main landing gear is hydraulically actuated to retract inboard into the fuselage. Each main landing gear is locked in the down position by folding lock strut and in the up position by an up-lock hook and mechanism. Shock strut doors close the opening in the wing for the main gear shock strut and drag strut. A wheel well seal closes against the main gear tyre circumferences, when the airplane is in the flight with gears retracted. . Lock mechanisms and sensors assure that the main gear is down and locked or up and locked. Manual extension is available in case of a hydraulic system malfunctions.

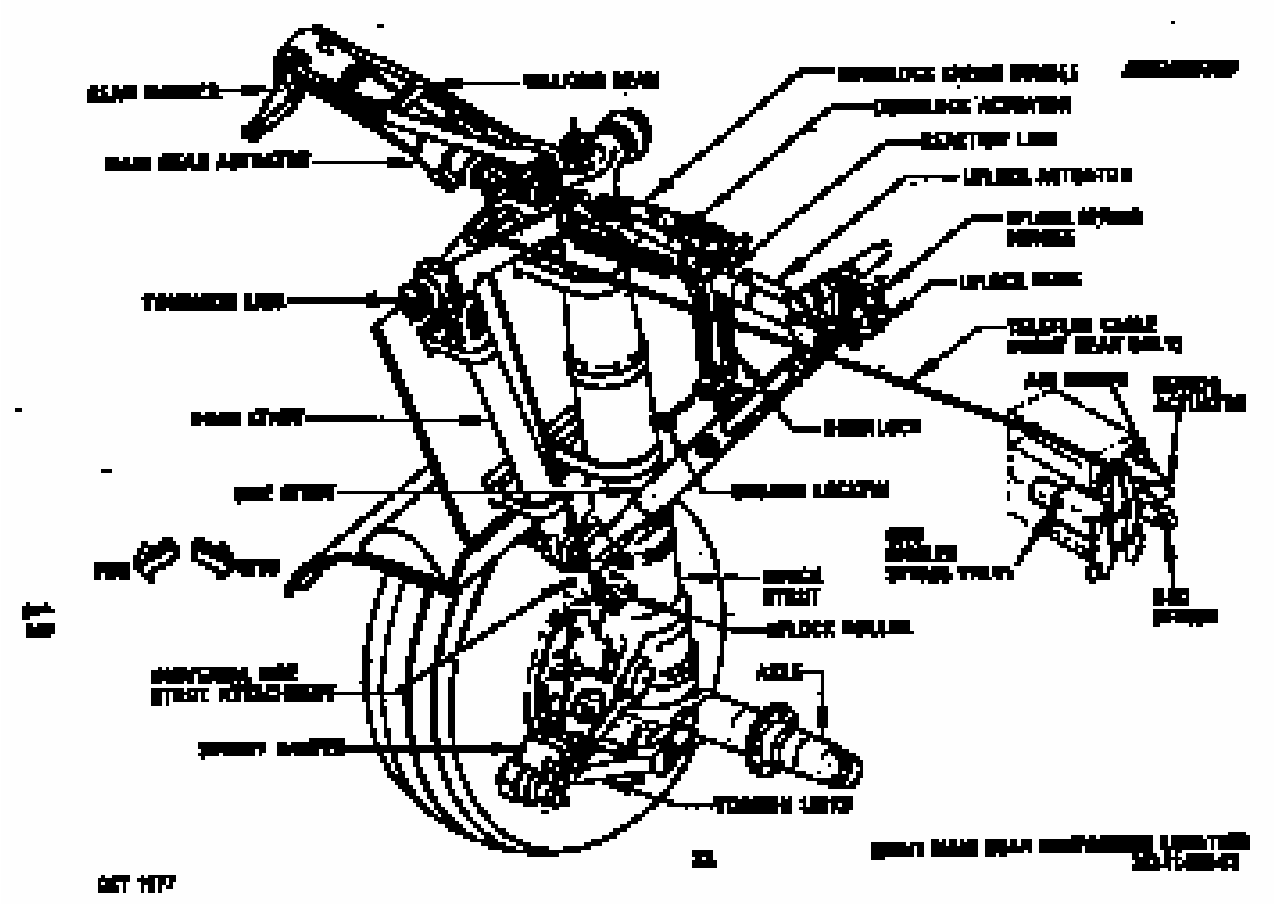

Fig 3. Landing Gear Shock Strut Assy.

The main landing gear structural components include a shock strut, drag strut, side strut, torsion link, and reaction link. The main gear shock strut is the primary supporting member of the landing gear. In addition to the structural components, the main gear wheels, tyres, and doors are an integral part of the main gear assembly. The brake unit is attached to the landing gear inner strut brake flange by means of ten bolts and nuts.

The braking system provides the means to control the airplane speed during parking and ground maneuvering, stop wheel rotation after take-off and shorten the landing run. A disc type brake is mounted on each of the four main gear wheels. The brakes are manually controlled by the Captain’s or First officer’s rudder brake pedal. Linkage between the rudder brake pedals provide a parallel input via cables to the dual brake metering valves. The brake metering valve port system hydraulic pressure to the respective wheel brakes.

The auto brake pressure control module delivers the hydraulic pressure as required by the selected deceleration, through the antiskid valves to the brakes, This brake function bypasses the brake metering valves and provides brake application with no pilot brake pedal input.

5.2. LANDING GEAR BRAKES;

Each main gear wheel is fitted with a brake unit. It is a multidisk type consisting of five rotating and six stationary frictional elements. Two of the stationary disks, i.e. pressure plate and backing plate are lined on one surface. The remaining four stationary discs i.e. stators are lined on both surfaces are notched on the inside diameter to enable them to fit and slide axially on the torque tube splines. The lining are made from an inherently heat stable ceramic material, that will maintain its original strength and friction ability t incandescent temperature. The rotating disc i.e. rotors are keyed to the wheel. Each rotor consists of seven solid steel segments that are secured to a spider with keyed straps. The brake carrier houses six pistons those are interconnected through drilled passages and six automatic adjuster assemblies.

5.2.1. DATAS;

Brake weight (Appx.)	74.8 Kg
Size and type	350.8-208.0 mm, 5-rotor brake
Number of brake assemblies	Two per gear/ four per aircraft
Rotors	segmented steel
Linings	Trapezoid shaped cerametalic
Torque tube	Steel
Piston housing	Forged aluminum
Operating pressure	20685kPa
Brake running clearance	2.08 mm

5.2.2. Description:

The main landing gear brake assembly is a size 350.8-208.0 mm hydraulically actuated, five rotors multiple disc type brake. The disc elements of the brake assembly are housed in as area between a hydraulically operated piston housing assembly and a torque tube and backing plate assembly, which is bolted to the piston housing. The brake assemblies are interchangeable on any position of the aircraft main landing gear.

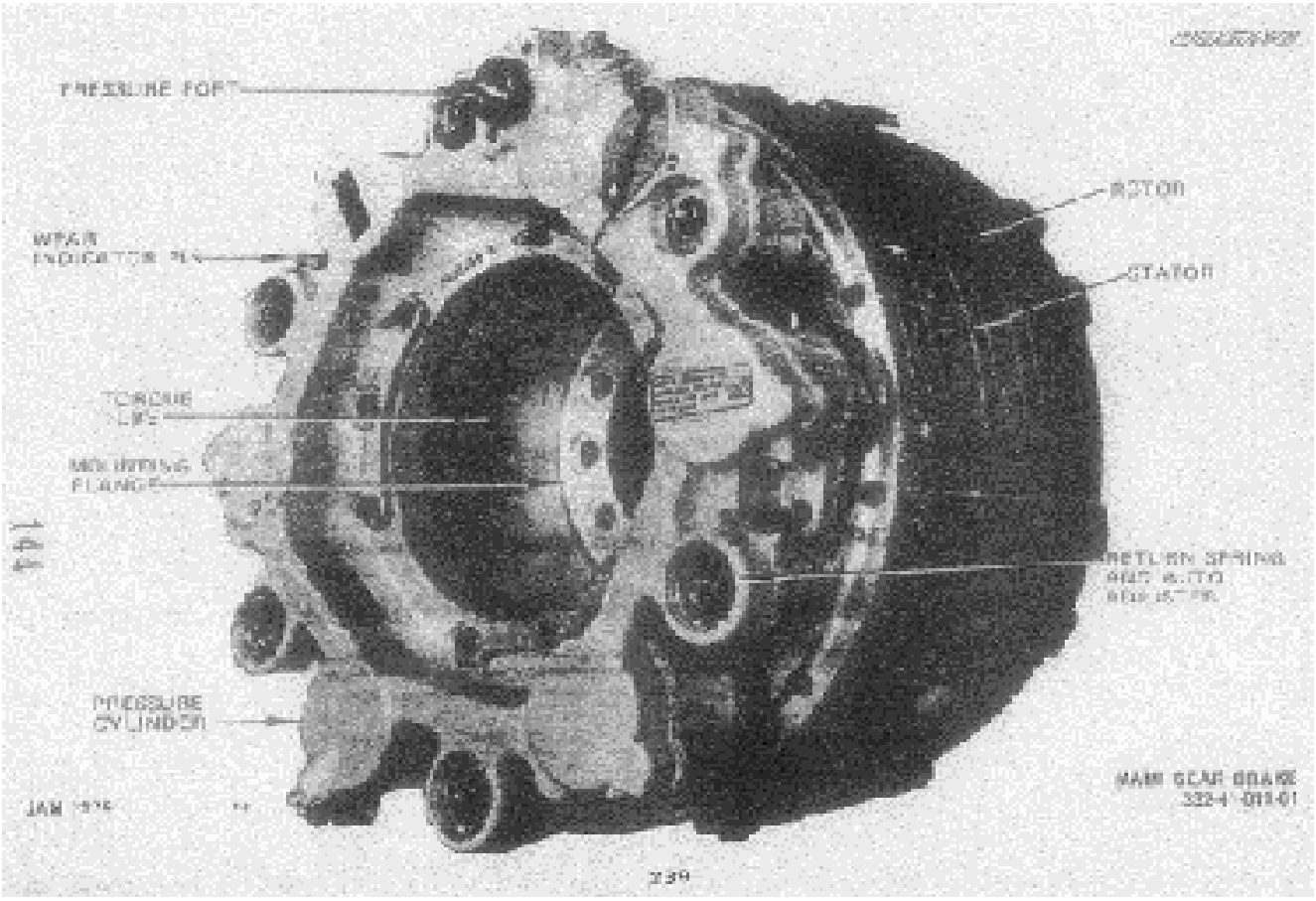

Fig 4. Main Gear Brake

The rotating disc elements (rotors) of the brake assembly are of the segmented design. Each rotor assembly consists of seven steel segments mounted on a spider-type structural ring. The segments are retained as an assembly by riveted steel straps around the outside diameter. The rotor spider is slotted and serves to engage the rotor drive keys of the wheel assembly during operation.

The break stationary elements (Pressure plate, stator plates, and stator torque tube backing plate), serve as brake lining carrying members. The trapezoid shaped brake lining is made of a compound of inherently heat –stable ceramic and metallic ingredients, balanced to retain strength and frictional properties at incandescent temperature. The pressure plate and backing plate sections of the stator torque tube replaceable lining on their inner surfaces. Stator plates are positioned between each assembly, and both surfaces of the stator plates are fitted with replaceable linings riveted back to back. The pressure plate and stator plates are slotted on the inside diameter to index with and slide axially on the splines of the stator torque tube.

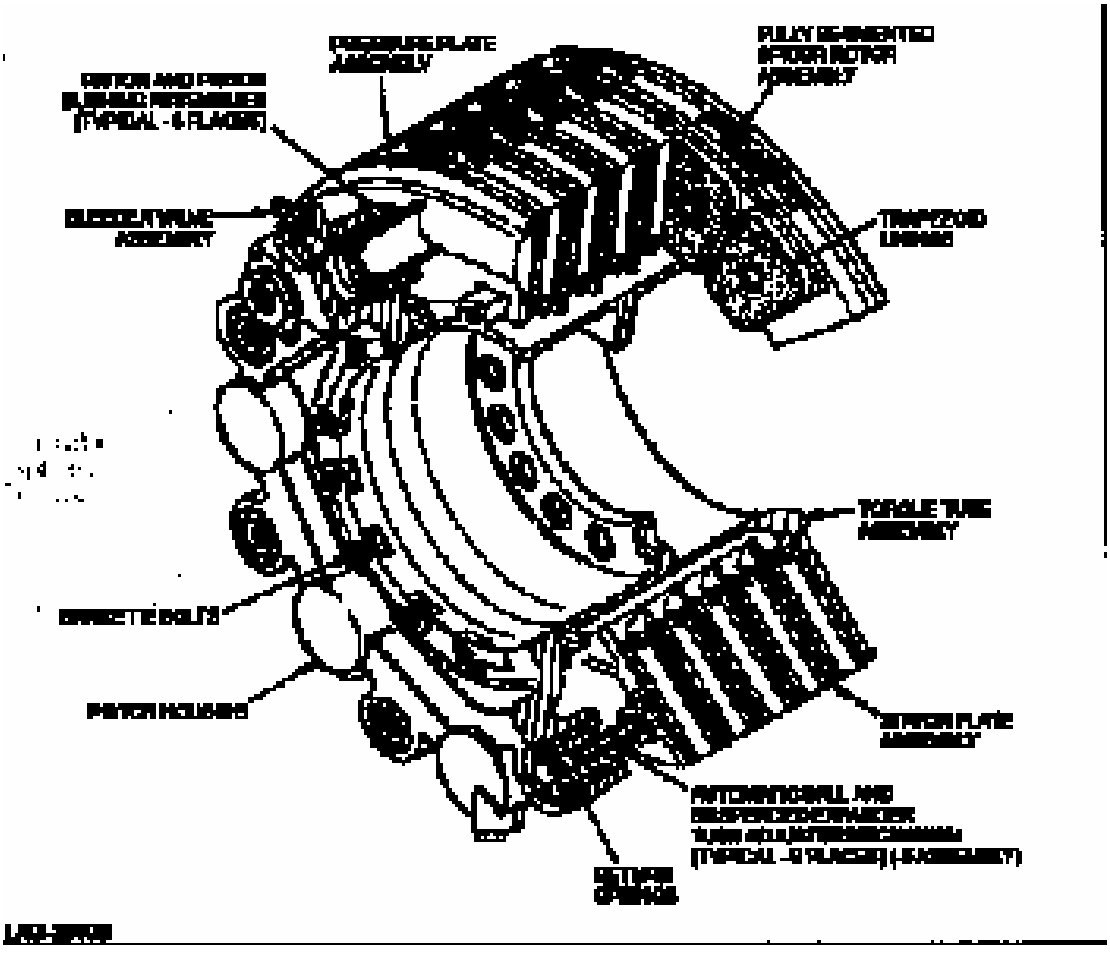

Fig 5. Cut Away view of Main Gear Brake

The break piston housing contains six equally spaced piston and bushings assemblies that are interconnected by drilled passages. The six combination return spring and automatic adjuster assemblies are housed in the piston housing, and are attached to the pressure plate by adjuster pins. The piston housing assembly provides a bleeder valve assembly to effectively remove entrapped air during installation and servicing.

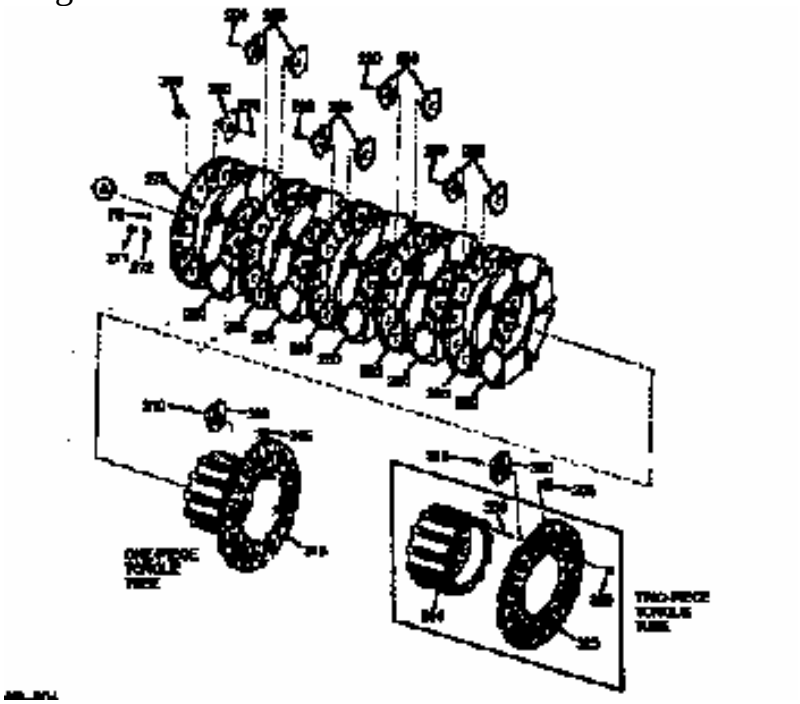

Fig 6. Main Gear Assy. Exploded View

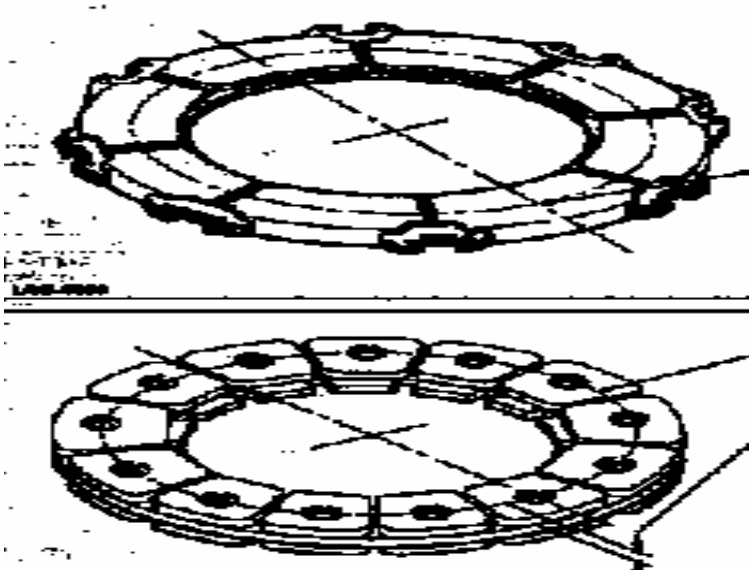

Fig.6(a). Brake Unit Rotor and Friction Plate.

Two lining wear indicator pins, attached to the pressure plate, provide a visual indication of the wear remaining in the frictional brake elements. When the end of the lining wear indicator pin is flush with the top of the guide bushing in the piston housing with parking brake pressure applied, the brake must be removed from the aircraft and disassembled for inspection.

5.2.3. OPERATION

The brake assembly is normally operated by fluid pressure from the aircraft main hydraulic system. Actuation valves through linkages and pushrods control brake operation when the brake pedals are depressed.

When brakes are applied, hydraulic fluid under system pressure enters the inlet port of the brake and is distributed to the six brake pistons through interconnected drilled passages in the piston housing. The fluid pressure moves the pistons outward against the pressure plate, which presses the stators and rotors together against the backing plate. Rotational friction, generated between the stationary lined plates and the brake rotors, provides the required braking.

The piston housing is attached to the pressure plate by six adjuster pins mounted through return springs. In the –4 brake, these pins are retained by a friction bushing. When brake pressure plate is applied, the pressure plate moves away from the piston housing causing the adjuster pins to compress th return springs.

CHAPTER-6

EXPERIMRNTAL WORK AND PROCEDURES.

The purpose of the present study is to introduce a stochastic method for the analysis of friction and wear test results for the design of brake pads in order to test analysis process. The aim of this experimental work is to carry out wear behaviour of the aircraft brake friction pads and analyses the wear rate of different models as explained below, so as to enhance life of the brake friction pads

6.1. Collection of data:

On field survey of the brake units fitted on the aircrafts are carried out and revealed that the range of operating life of the brake friction pads differs substantially.

---------Number of aircraft landings----------

Brake unit serial no.	1	**2**	**3**	4	5	6	7	8	9	10	Average
C-0005	556	554	1470	449	924	692	550	622	635	1172	522.1
C-0007	519	464	673	472	540	421	345	555	648	584	522.1
C-0315	526	822	534	573	634	460	354	632	343	476	535.4
C- 317	519	1078	561	305	821	623	579	1105	715	820	712.6
C-0319	1177	479	686	448	663	1212	573	518	537	521	677.8
C-0232	596	509	634	592	630	483	1048	832	880	707	691.1
C-0355	379	600	959	517	548	432	696	618	670	954	637.3
C-0356	540	599	802	409	523	779	521	627	597	1461	685.8
C-0037	501	673	706	580	408	899	598	367	07	1254	649.3
C-0038	822	577	605	332	695	474	888	629	634	552	620.8

Randomly collected data of ten brake units fitted of different aircrafts, from their history card for last ten total worn out conditions. Following are the list of data for total worn out life of the ten brake unit friction pads in terms of number of aircraft landings.

6.2. ANALYSIS OF THE DATA

From analyzing the above data, it is found that the minimum life of the brake unit in terms aircraft landing is 343 and the maximum life is 1470. The range of the above data for life of the friction pads is very high. In the case of high energy stop of the aircraft due to short runway, abandoned take off etc. the friction pads worn out more as compared to low energy stop of the aircraft. Hence an attempt is made to increase the life of the friction pads for high-energy stop of the aircraft. As the friction pads of the brake unit s are being manufactured and supplied by Hindustan Aeronautic Limited, a reputed company and is being standardized and approved by Director General of Civil Aviation, hence it is assumed that the composition of material of the friction pads are optimized. Hence to improve the life of the friction pads design aspects of the pads are considered. In case of high-energy stop, the kinetic energy of the aircraft speed is converted into heat energy between the rotors and friction pads of the brake pads and the interfacial temperature becomes very high. This interfacial temperature has direct bearing on the wear of the friction pads. So cooling the interface between the rotors and stators can increase life of the friction pads. Hence making radial grooves on the rubbing surface of the friction pads can exist air flow between the rotor and the friction pad, there by reducing the inter facial temperature.

6.3 *Study of Brake Lining Materials of Boeing 737-200 Aircraft by Minor Geometrical Changes in Design of Pads for Better Cooling*

During the landing of an aircraft i.e. at the touch down instant, aircraft has a vertical (sink) velocity and a horizontal (glide) velocity. The glide velocity causes the air vehicle to run forward on the runway and brakes have to be applied to bring it to a stop. The landing distance has significant operational, economical and military applications. A short run improves the versatility of the aircraft in respect to the size of runway it can operate from. Military aircrafts often have to take off and land on badly prepared and small runways. A short landing run is imperative for the deployment of planes from aircraft carriers. The designers strive to have as short as possible operating runways. The length of the landing run depends on the way in which the braking is applied. When the braking force is low the stopping distance is long, and a stronger braking gives a shorter landing run up. The maximum brake force sustainable is dependent on the frictional forces at the interfaces of wheel and track. If braking induces a greater moment on the wheel, the wheel stops rolling and starts to skid on the track surface [29]. In this condition destabilizing forces come into play due to loss of rolling motion. Thus, to achieve the optimal landing run (the shortest stopping run without skidding), the braking force has to be varied to match the frictional force at all runways. The stopping/slowing distance requirements are now becoming even more stringent with increase in operating speeds of aircrafts. Therefore, frictional brakes for aircrafts require steady, repeatable and effective stopping behavior under a range of operating temperatures and environments.

Brakes must perform reliably under hot, dry, wet, or cold conditions [30]. In addition to this, it is essential to have longer life of brake lining material in order to keep maintenance cost low. To predict the wear of brake lining materials in

laboratory, there are a variety of bench-scale tests in use. But most are criticized for not correlating very well with the kinds of wear that the materials experience in service [3,4]. The error in wear prediction in laboratory occurs due to inability in simulation of field working conditions while conducting tribo-testing of brake materials.

Indian Airlines operates Boeing 737-200 aircraft in disturbed area (J & K and North-East) of country for carrying military as well as civilian people. Due to security concerns, the small landing runways are being used in disturbed areas in comparison to peace regions. Shorter runway is leading to about 50 to 60% less life of braking pad. It is clear that stoppage of Boeing 737-200 aircraft within small runway causes application of high friction forces, which might be resulting in significant temperature rise at the interfaces. This phenomenon accelerates wear of brake lining materials. Therefore, it is expected that cooling of the brake interface is essential to minimize the wear of contact. Hence, the purpose of present work is to study the wear of brake lining material of Boeing 737-200 aircraft in laboratory by minor geometrical changes in design of pad for better cooling at environmental conditions of Delhi. Four separate designs (Design-I, II, III, and IV) in braking pads have been conceived for providing better cooling at contact of brake lining material and counter-surface. For Design–I of pad, the measured wear of lining material is less in comparison to other pad designs. Therefore, measurement of the wear characteristics at interfaces has assessed better cooling for Design-I.

6.4. COLLECTION AND PREPARATION OF THE MATERIALS FOR THE EXPERIMENTAL WORK.

Few friction pads and the rotor plate of the brake unit of Boeing 737-200 aircraft are collected from the assembly shop of the brake units.

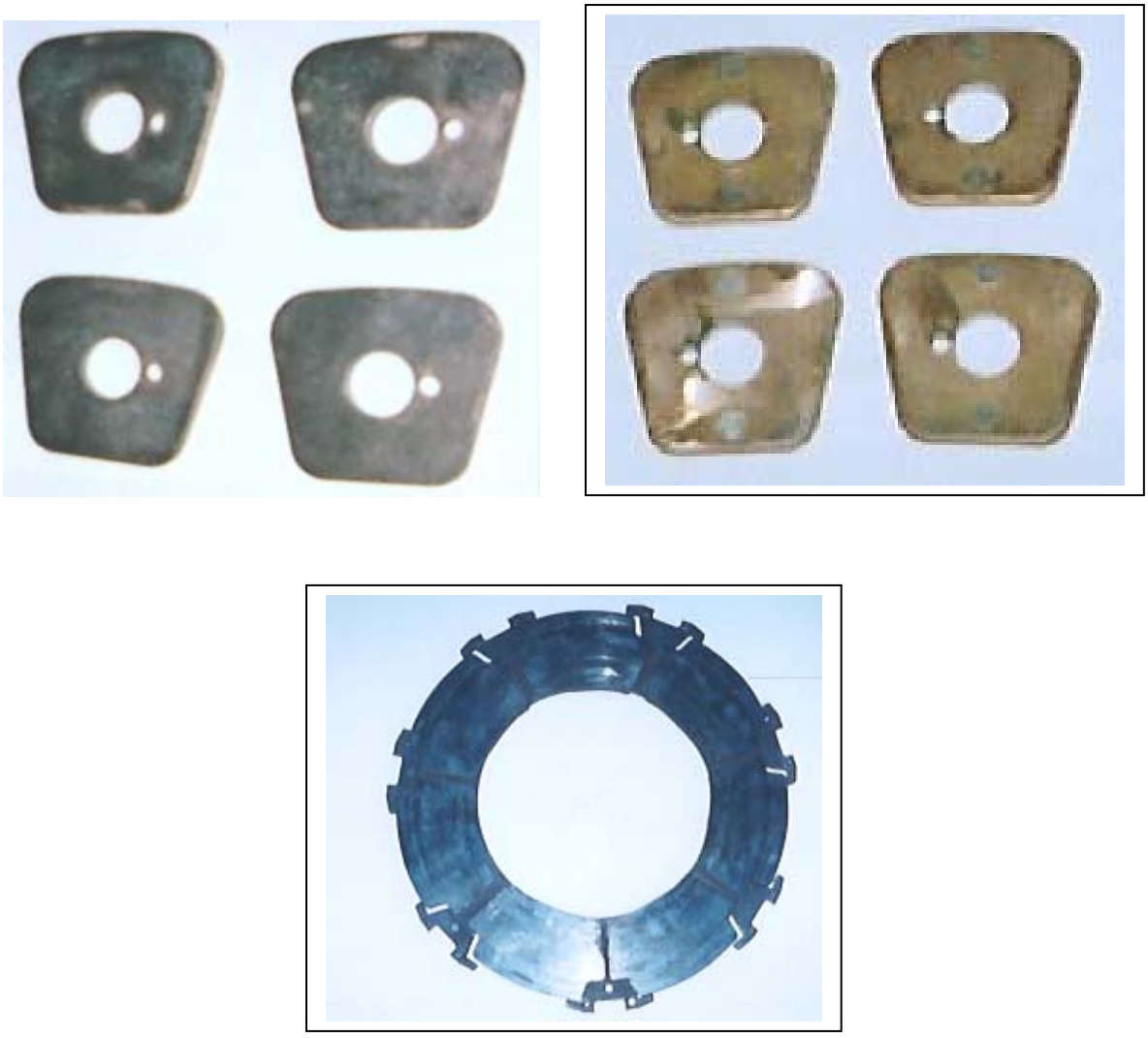

Fig.7. *Rotor and friction pads of aircraft brake unit*

To test these specimens on the ‘Pin- on- disk’ tester, four friction pads and one segment of the rotor plate are fabricated to their shape as per the following drawing shown in the figure.

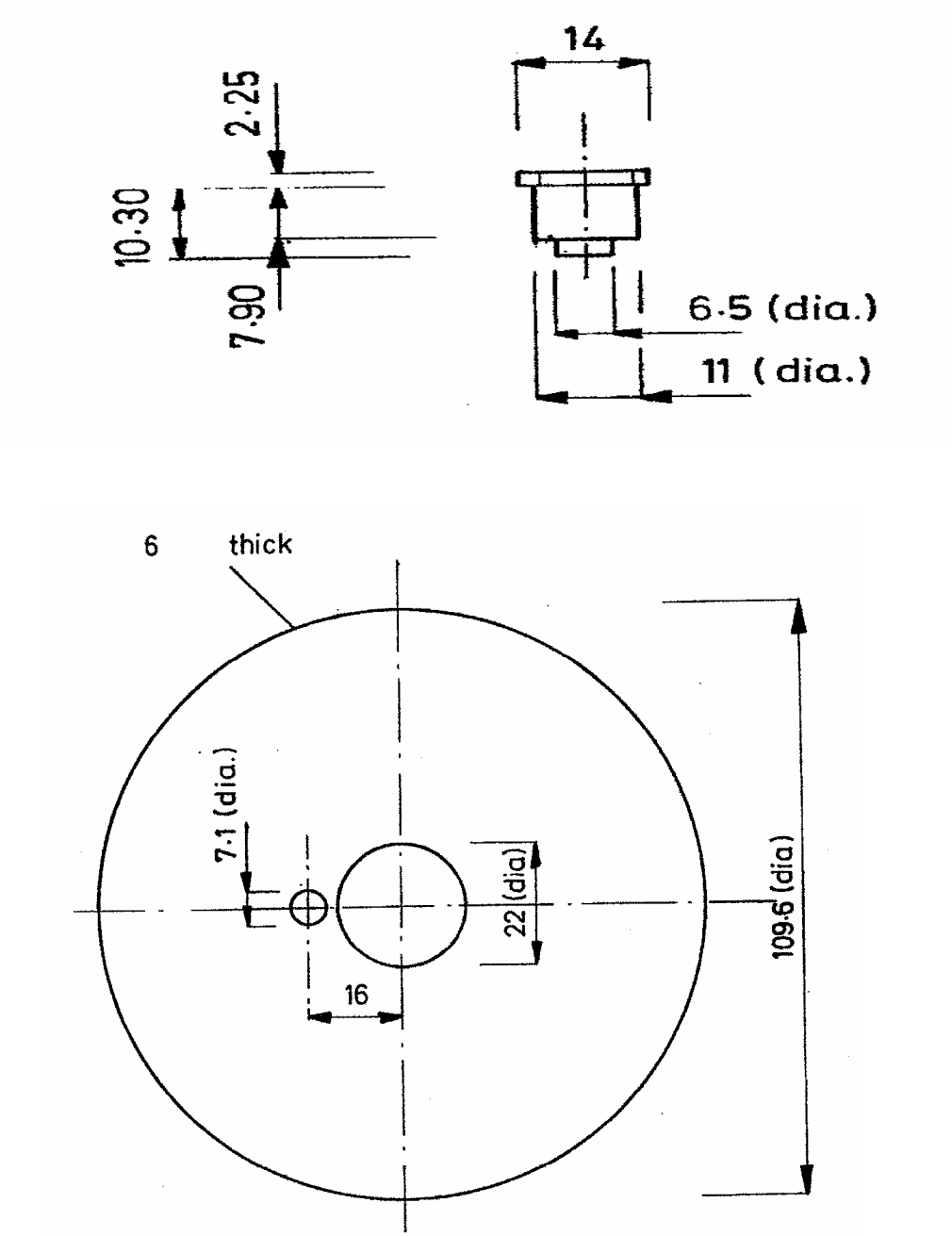

Fig.8 *Drawing for manufacturing disk and slider.*

Fig.9 *Manufactured sliding pin and separation of one segment of the Rotor plate along with the friction plates.*

Sliding pins are made from one segment of the rotor plate, so that material of the pin on surface of the specimen does not differ to the actual materials.i.e material used for rubbing on the disc for testing is the same material used on the brake unit. The above figure shows the dimensions for making the pin and disk.

6.5 TEST RIG.

Following figure shows a test rig of 'Pin- ON- Disk' type tester. A fabricated friction pad is attached to a disk support and was rotated by a variable AC motor through an electrical cluch. The manufactured disc is of thickness 6mm. The slider has a circular sliding surface of k6.5 mm diameter and is being fabricated from the rotor material. The rotating disk was disconnected from the rotor by a clutch before the slider was pressed against a disk surface at a radius of 16 mm. A load of 10 N was applied to the slider by means of a dead weight. The

friction torque exerted on the slider is measured by a load cell. The disk rotation speed was kept constant and was measured by an electrical speed counter.

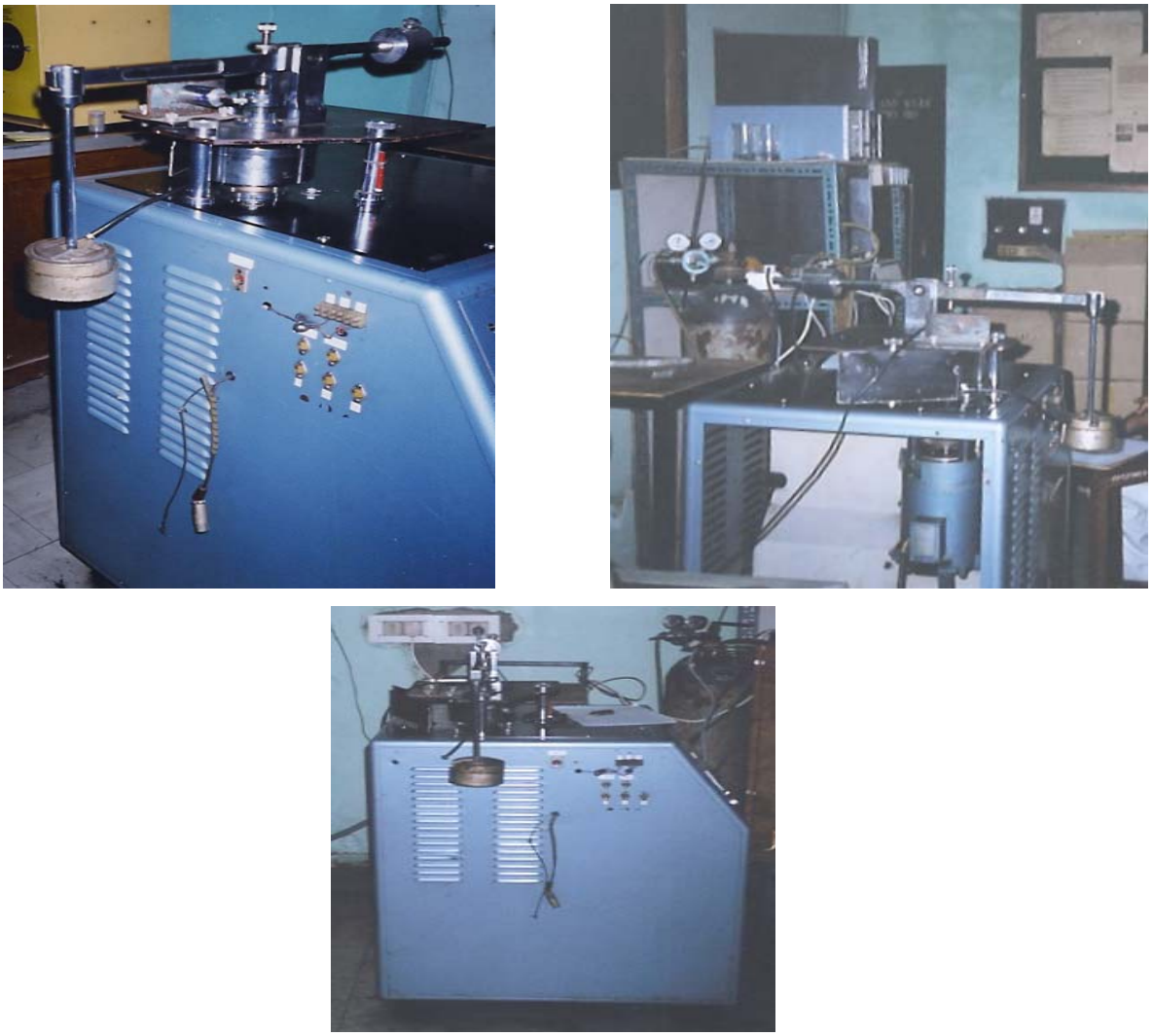

Fig.10 *'Pin-ON-Disk' type test Rig.*

6.6. SLIDERS

One segment of the rotor is detached from the rotor plate by drilling out the locking rivets. From that segment parallel rods are cut and sliding pins are made to their dimension with the help of a lathe machine.

Fig.11 *Manufactured sliding pins.*

Fig.12 *Rotor plate after removing one segment Friction plates are placed above the plate*

6.7 DISKS

Disks are manufactured to their dimensions from the collected friction pad to their dimension as per the above drawing. Four models of disks are prepared making two, three and four equidistance radial grooves on the rubbing surface of the friction pads. Sample1-four grooves, Sample II- two grooves, Sample III- three grooves and Sample IV- plane.

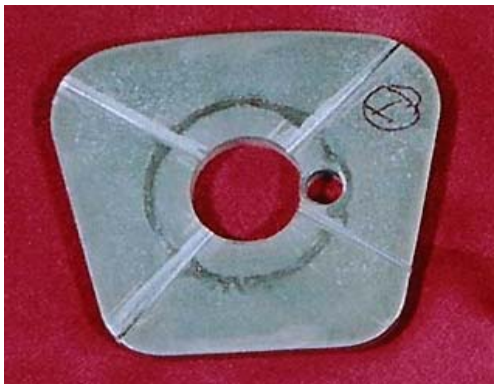

Fig.13 Sample-I
(Friction plate with four slots)

Fig.14 Sample-II
(Friction plate with two slots)

Fig.15 Sample-III

(Friction plate with three slots)

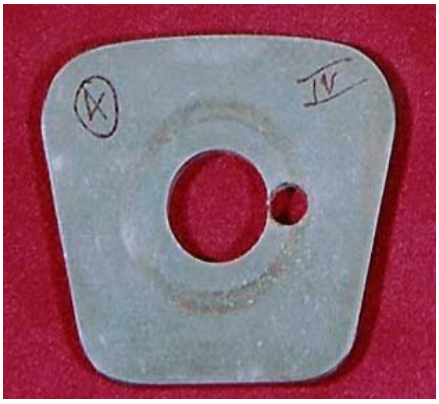

Fig.16 Sample-IV

(Friction plate with plane sliding surface)

6.8. TEST CONDITIONS.

The series of experiments were performed on all the four samples of friction pads at constant room temperature under the condition of constant r.p.m., constant load and equal time period for each sample. The wear behaviour of the samples are conducted at 60 r.p.m., load= 10 N and for a time period of 60 minutes. Each sample is weighed before and after the test and the difference of weight is calculated as weight loss.

After the test the rubbing surface of each sample is scanned in a scanning electron micrograph (SEM) with 300 magnifications for a length of 10 mm. Following are the pictures of all four samples after magnification.

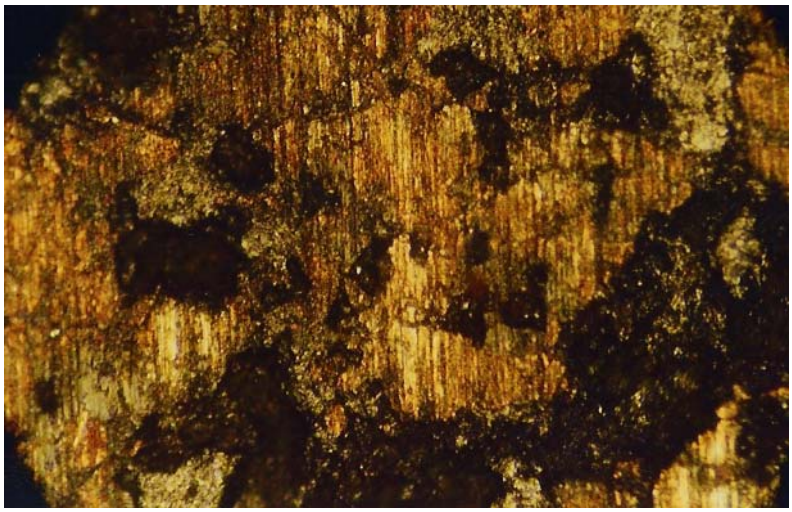

Fig.17 *General surface texture (300 x magnification) of sample before test*

Scanning electron micrographs of the specimen before testing on the test rig, as shown in the above figure, heavy black patches on the surface indicates flickering and fragmentation of chips and very rough topography.

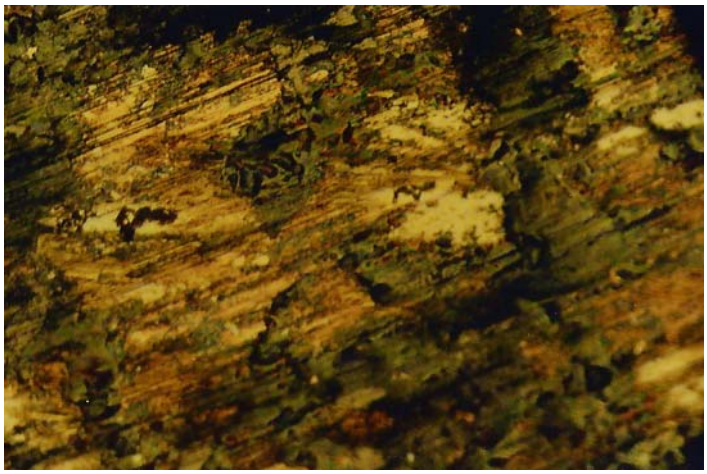

Fig.18 *Surface texture (300x magnification) of sample-I after test (Load=10 N, Track dia=32 mm, rpm=60, time=1 hour)*

Scanning electron micrographs of sample-1 (with four slots) shows the surface is more compact, smoother smeared appearances in the wear track were observed.

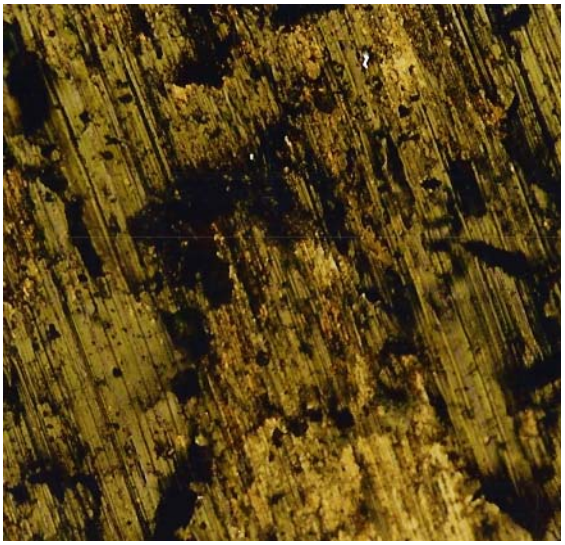

Fig.19 *Surface texture (300 x magnification) of sample-II after test (Load=10 N, Track dia=32 mm, rpm=60, time=1 hour)*

Analyzing the surface texture of the sample-II (with two slots) with scanning electron micrograph shows the heavy black spots indicating very rough topography. Scratches on the surface show that the ceramic particles are ploughed

out and dragged on the surface texture during the test. But these scratches are of not heavy as compared to the sample- IV.

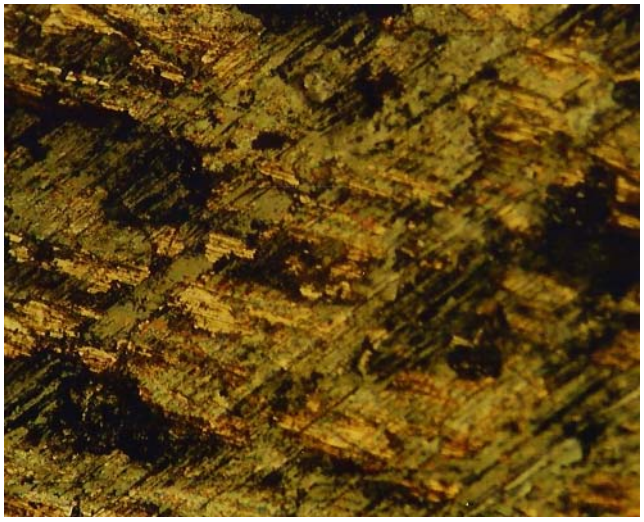

Fig.20 *Surface texture (300 x magnification) of sample-III after test (Load=10 N, Track dia=32 mm, rpm=60, time=1 hour)*

Scanning electron micrograph of surface texture of sample-III (with three slots) shows the surface is more homogenous, less dark spots and very light scratches as compared to sample-II and sample-III.

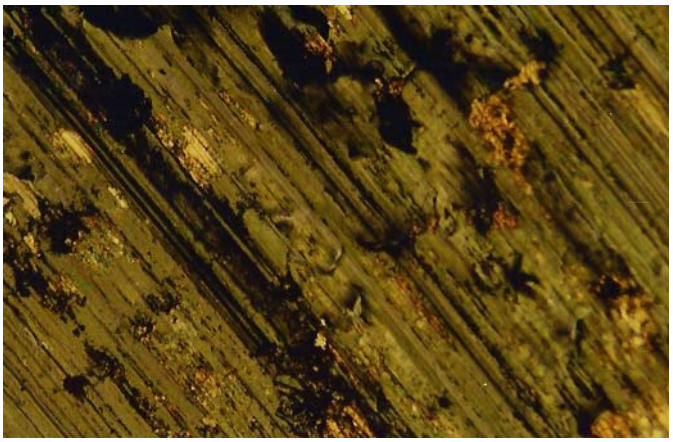

Fig.21 *Surface texture (300 x magnification) of sample-IVafter test (Load=10 N, Track dia=32 mm, rpm=60, time=1 hour)*

The above picture shows the scanning electron micrograph of sample-IV after test reveals that many rough regions and was. plastically deformed with a plugging appearance characteristics of adhesive wear. The rough regions represent the severe wear. Heavy scratches on the surface shows that the ceramic particles are ploughed out and during sliding, it removes more particles in form of scratches as in the case of three body abrasion wear.

6.9 DISCUSSION

To understand the abrasive wear behavior of ceramics under different test conditions, many test were carried out for all four samples and parameters of surface topography are recorded.

The surface roughnesses of the profile of the samples are in terms of the following parameters and are tabulated as follows.

Parameters	Sample-I	Sample-II	Sample-III	Sample-IV
R_a (μm)	2.2449	1.4019	4.0693	1.2480
R_q(μm)	3.5037	2.0137	5.1159	2.2931
R_p (μm)	3.2020	3.7146	6.1055	3.0020
R_v (μm)	13.1273	8.2265	15.3917	10.9821
R_{sk}	-2.5419	-1.5628	-1.2090	-3.1818
R_{ku}	10.0833	6.5424	3.5583	15.2726
R_z (μm)	16.3293	11.9410	21.4972	13.9822

Weight Loss of pads

Sample-I (Four slots)=0.0014 gm

Sample-II (Two slots)=0.0024 gm

Sample-III (Three slots)=0.0018 gm

Sample-IV (Plane)=0.004 gm

Where

R_a = Arithmetic mean of the departures of the profile from the mean line

R_q = Root mean square of the ordinates

R_p = Maximum height of the profile above the mean line within the sampling length

R_v = Maximum depth of the profile below the mean line within the sampling Leng+th

R_s = Skewness is measure of symmetry of the amplitude distribution curve about the mean line

R_{ku} = Kurtosis is a measure of shape (sharpness) of the amplitude distribution

R_z = Sum of the largest peak and the largest valley of the profile within the sampling length

Variation of surface roughness i.e. center line average (R_a) of abraded surfaces of the models at fixed sliding speed of 60 r.p.m., under load of 10N and time 60 minutes.

Specimen	Surface roughness (R_a in μm)
Sample-I	2.2449
Sample-II	1.4019
Sample-III	4.0693
Sample-IV	1.2480

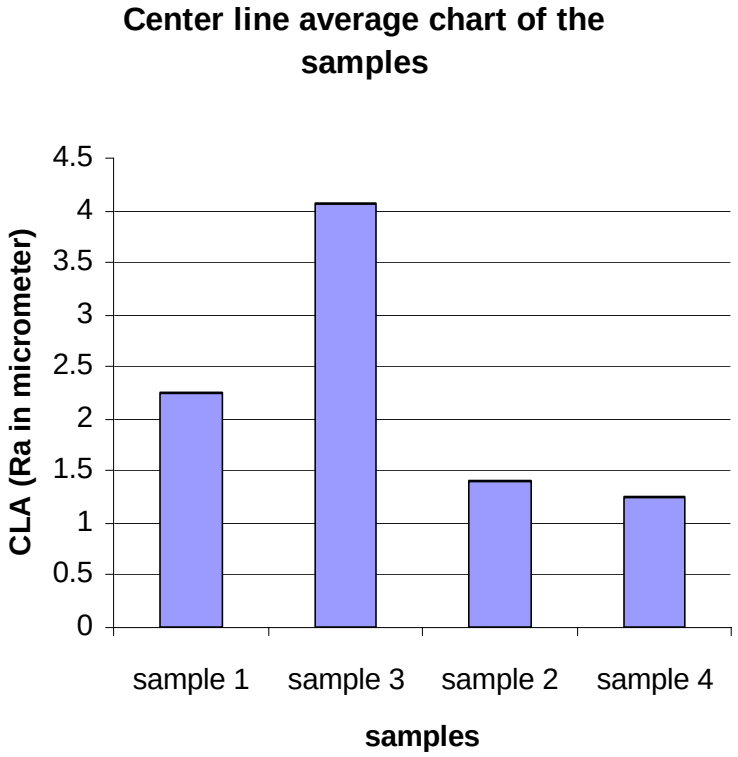

Fig. 22. Samples Vs CLA bar graph.

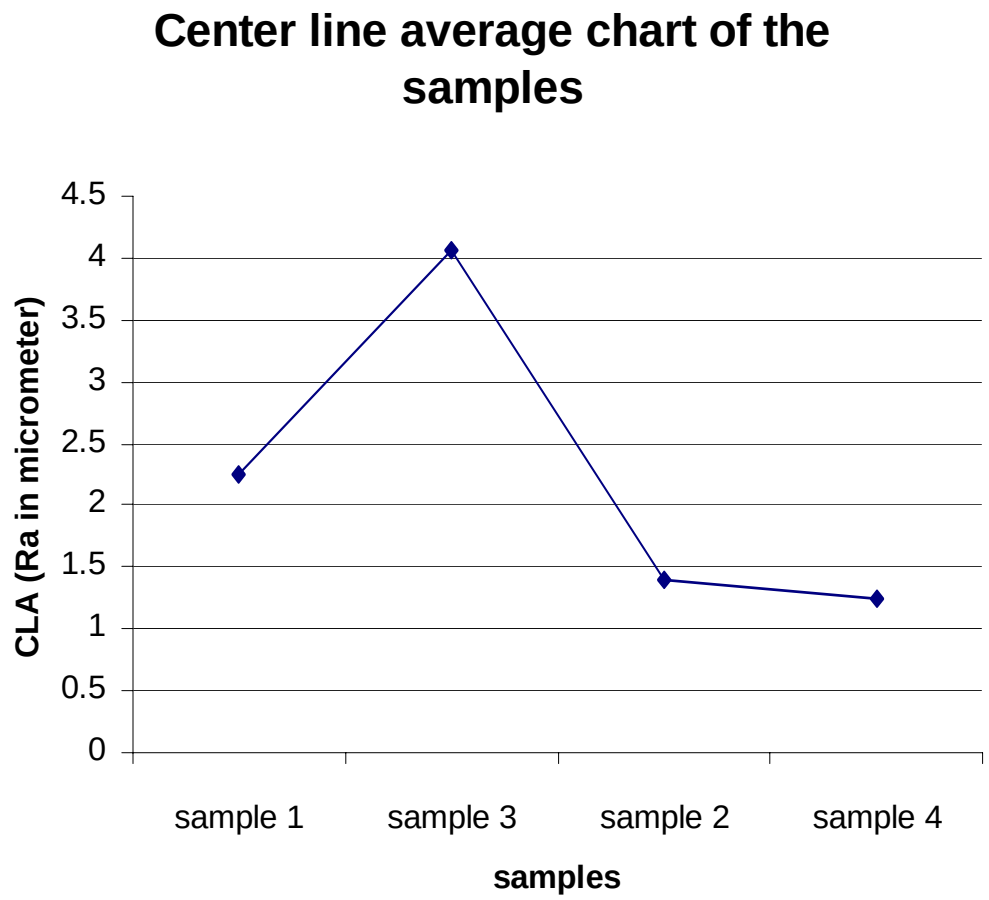

Fig, 23 Samples Vs CLA line graph.

The centerline average (Ra) value for the sample III is more than the others samples, signifies that the sample III has more compact granular surface texture than the other one. Analyzing the surface texture of sample III with scanning electron micro graph shows large number of flickering of the surface and also weight loss due test is more than that of sample I. Hence sample I has better surface texture than others.

Variation of surface roughness i.e. root mean square (Rq in μm) of surface texture of samples after test at fixed sliding speed of 60 r.p.m., under load of 10 N and time 60 minutes.

Specimen	Surface roughness (R_q in μm)
Sample-I	3.5037
Sample-II	2.0137
Sample-III	5.1159
Sample-IV	2.2931

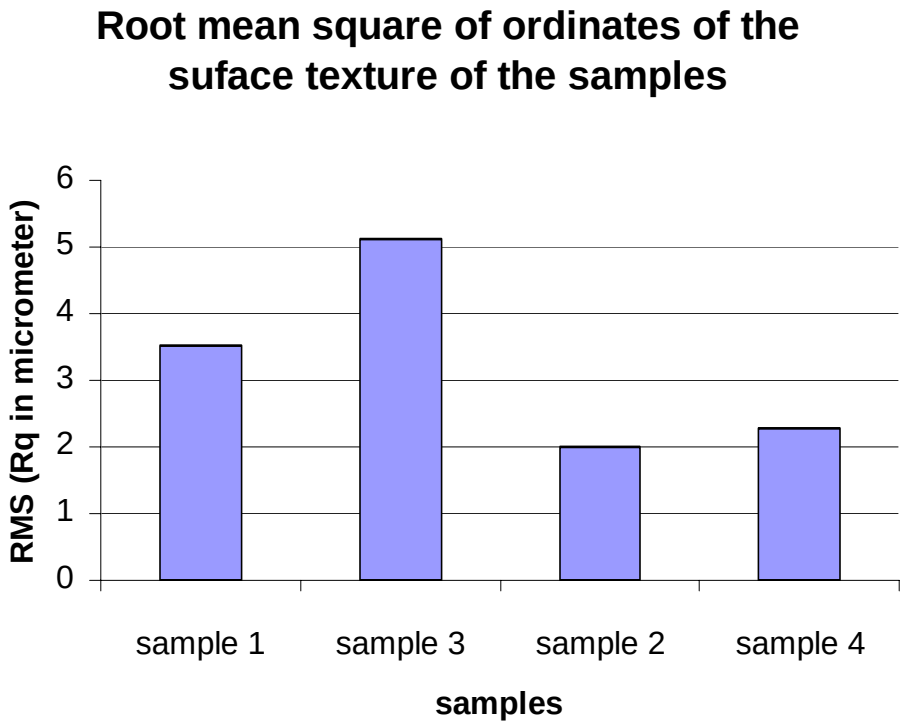

Fig. 24 Samples Vs r.m.s. bar graph.

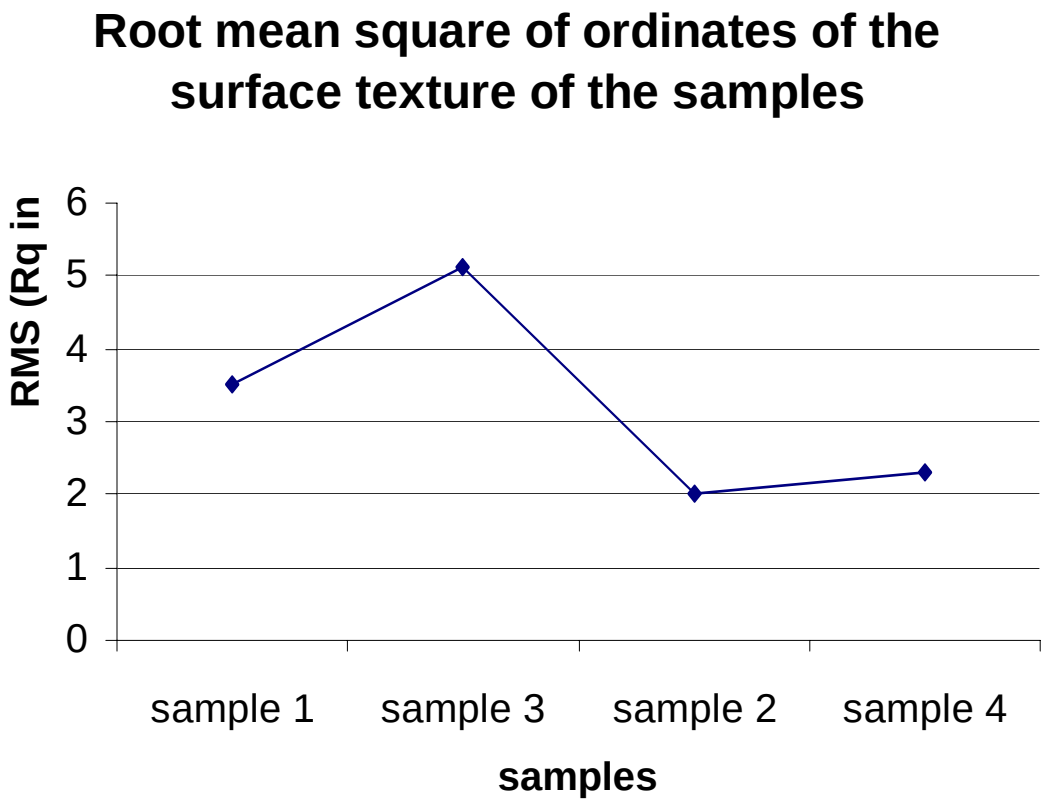

Fig. 25 Samples Vs r.m.s. line chart.

Root mean square of surface profile indicates the density of its microstructure. In this test though the r.m.s. value for sample III is more than that of sample I, still sample I has got better surface profile as seen in SEM of the profiles.

Variation of maximum height of the profile above the mean line (R_p in μm) of surface texture of the samples after the test at constant velocity of 60 r.p.m., load=10N, time=60 minutes.

Specimen	R_p in μm
Sample-I	3.2020
Sample-II	3.7146
Sample-III	6.1055
Sample-IV	3.0020

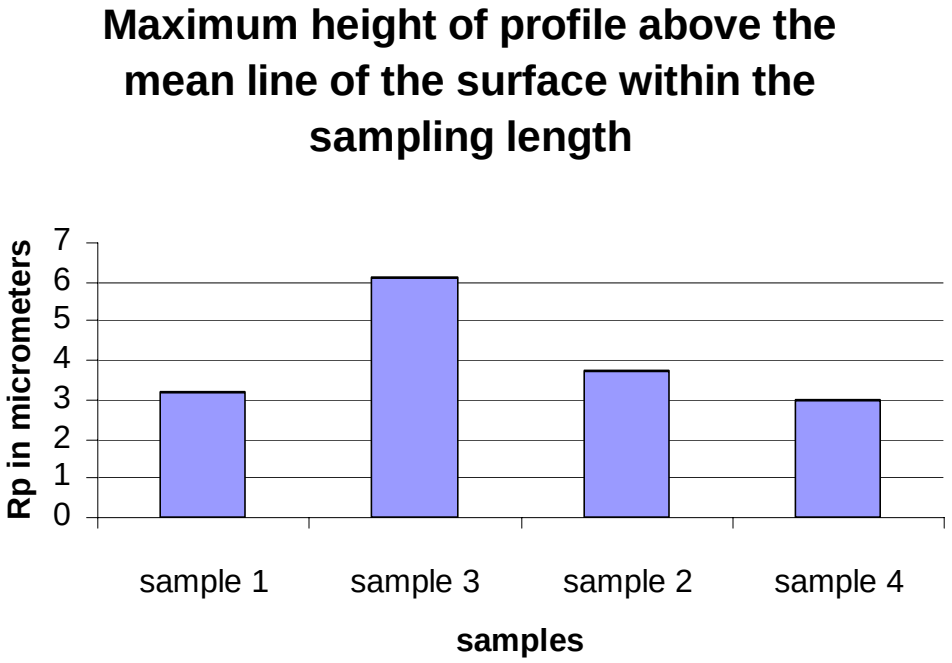

Fig. 26 Samples Vs maximum height of the profile above the mean line within the sampling length bar diagram.

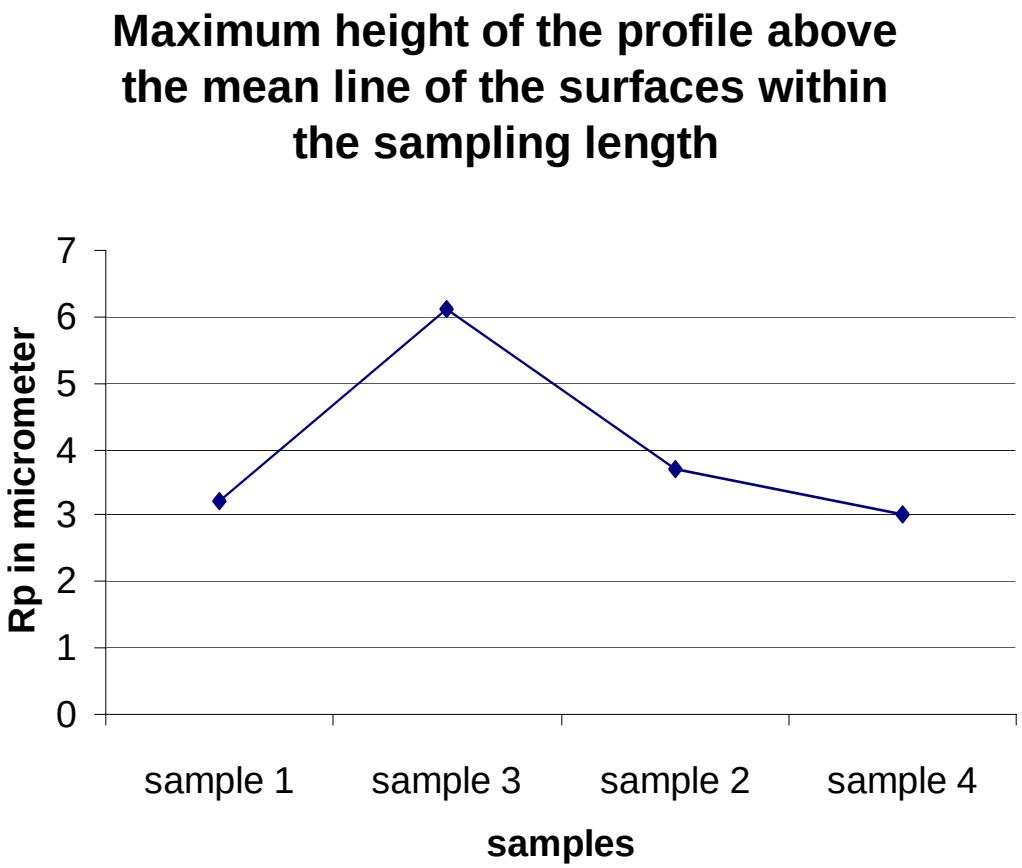

Fig. 27 Samples Vs maximum height of the profile above the mean line within the sampling length line diagram.

Studying the above two graphs shows, height of the profile above the mean line for sample III is more than the others. It indicates large number of valleys on surface texture hence rough profile. So sample I is preferable than the others.

Variation of maximum depth of the profile below the mean line (R_v in μm) of the surface texture of samples at constant speed of 60 r.p.m.,load=10N and time=60 minutes.

Specimen	R_v in μm
Sample-I	13.1273
Sample-II	8.2265
Sample-III	15.3915
Sample-IV	10.9821

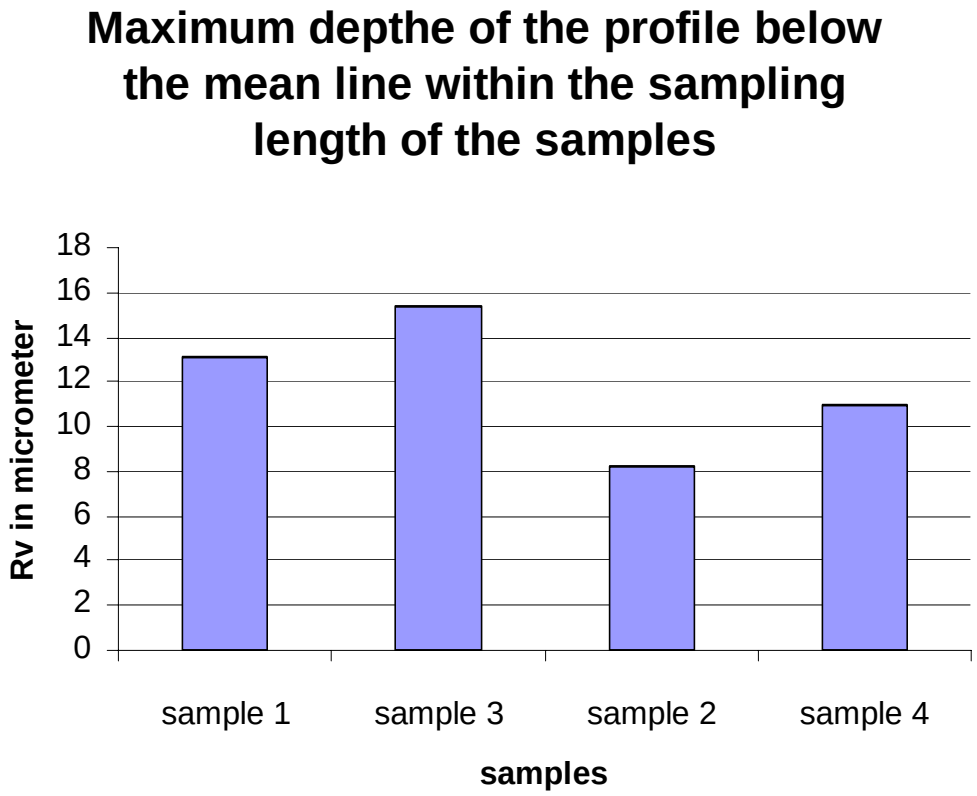

Fig. 28 Samples Vs Maximum depth of the profile below the mean line within the sampling length bar graph.

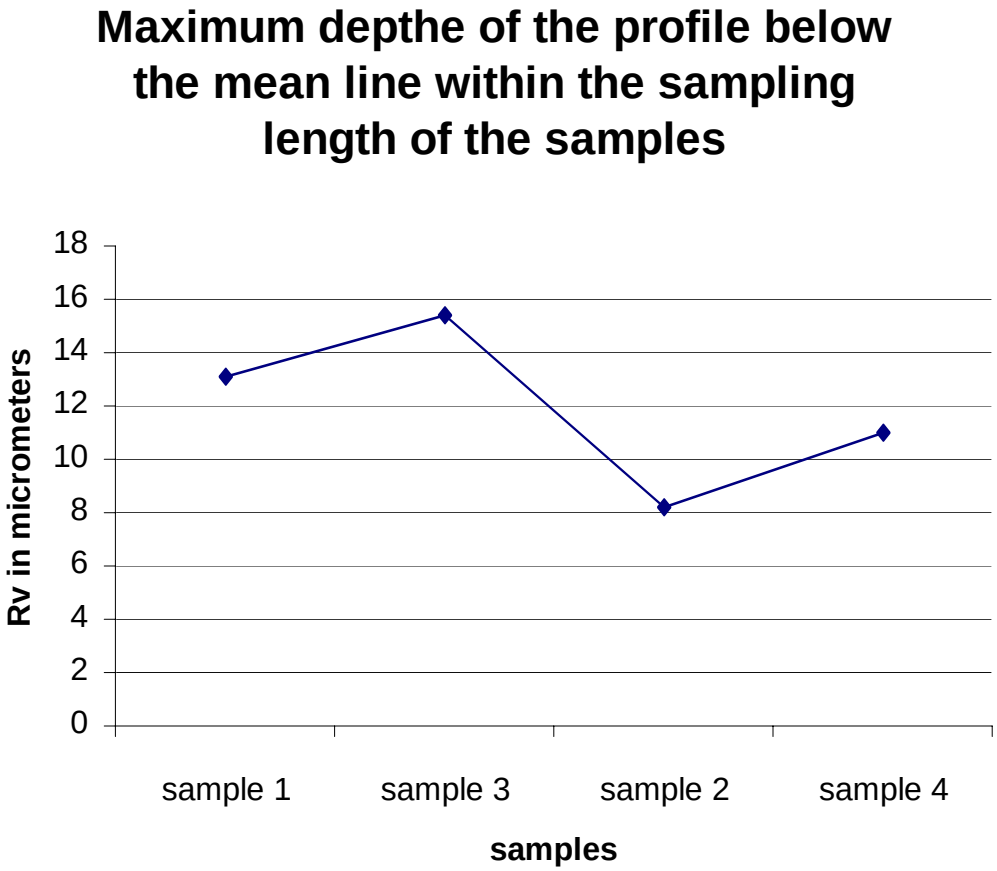

Fig. 29 Samples Vs Maximum depth of the profile below the mean line within the sampling length line graph.

The maximum value of depth of profile below the mean line for sample II is less than the others shows that the surfaces has got deep scratches than the other profiles. Sample III has maximum Rv as well as maximum Rp value hence it is more likely to have high wear rate than the sample I.

Variation of sum of the largest peak and largest valley of the profile (Rz in μm) of the samples at constant speed of 60 r.p.m., load=10N and time= 60 minutes.

Specimen	Rz in μm
Sample-I	16.3293
Sample-II	11.9410
Sample-III	21.4972
Sample-IV	13.9822

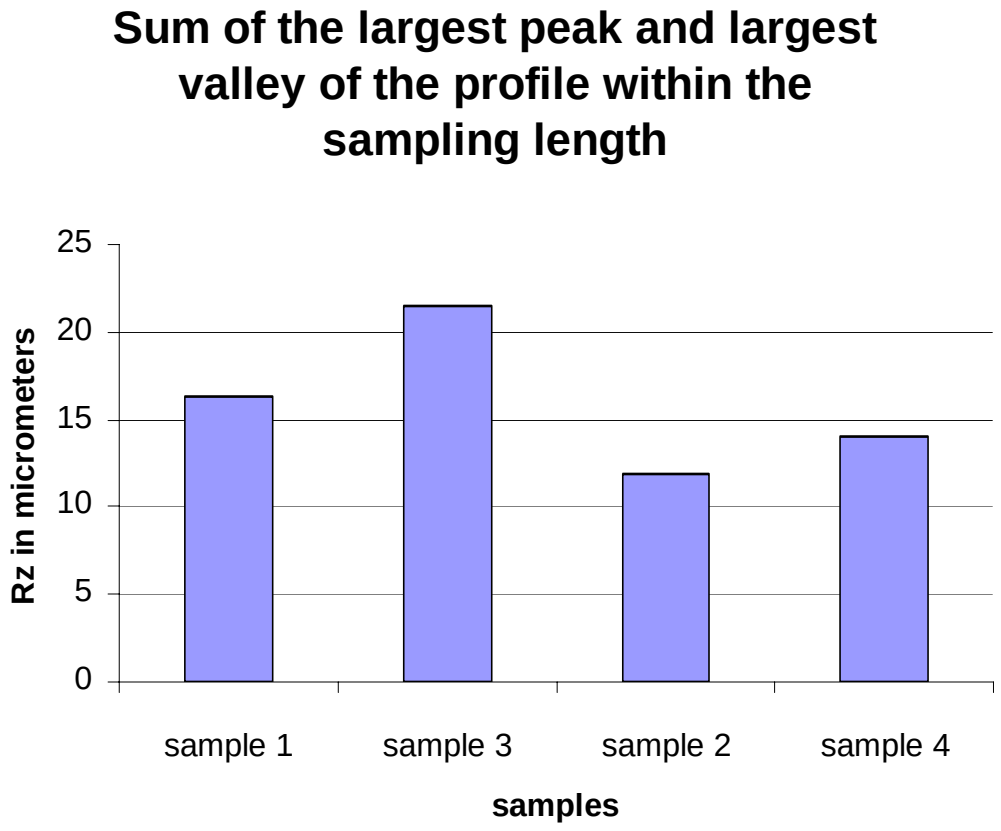

Fig. 30 Samples Vs Sum of the largest peak and largest valley of the profile within the sampling length bar graph

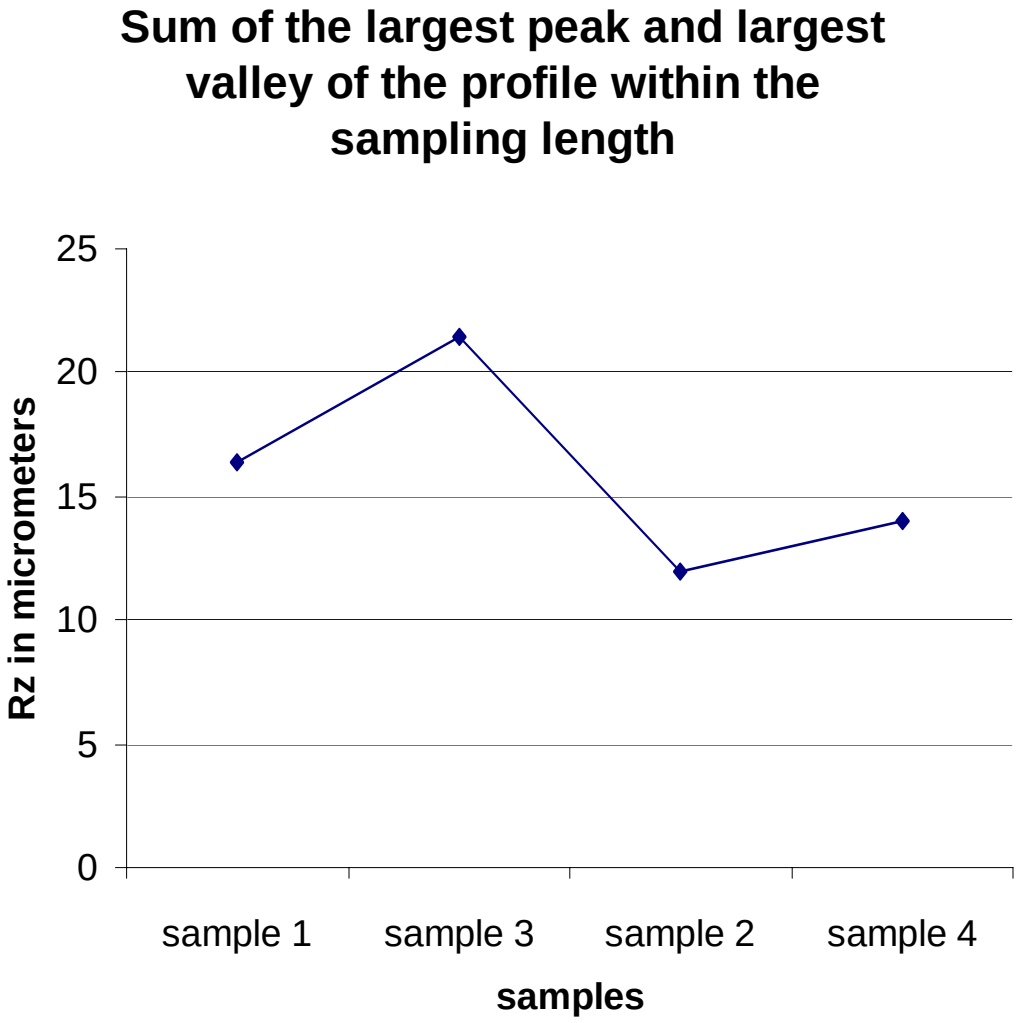

Fig. 31 Samples Vs Sum of the largest peak and largest valley of the profile within the sampling length line graph

Rz value for sample III is highest and for sample II it is lowest. Lower of Rz indicates less number of waviness of the structure profile where as higher value of Rz indicates the surface micro structure is porous hence wear rate is high.

Variation of skewness surface profile (R_{sk}) of the surface texture of the samples within the sampling length at constant speed= 60 r.p.m., load= 10N and time=60 minutes.

Specimen	Skewness
Sample-I	-2.5419
Sample-II	-1.5628
Sample-III	-1.2090
Sample-IV	-3.1818

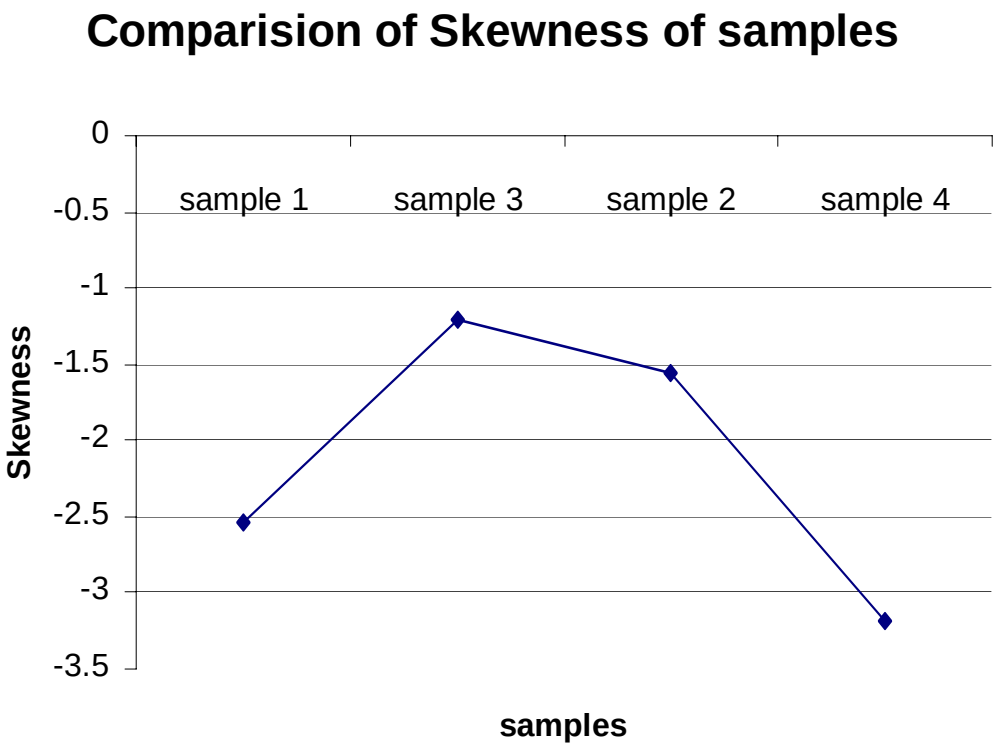

Fig. 32 Samples Vs Skewness line graph.

Positive skewness values predict higher contact force, real area of contact, number of contacting asperities, tangential and adhesion forces, while negative skewness values predict lower values and larger deviations from the Gaussian case. High negative value of skewness of the surface profile shows less wear rate. In this graph though sample IV has got highest negative skewness but due to third body abrasion the wear rate is high. Hence sample I is preferable than the other samples.

Variation of kurtosis of the surface profile (R_{ku}) of the surface texture of the samples within the sampling length at constant speed of 60 r.p.m., load=10N and time=60 minutes.

Specimen	Kurtosis
Sample-I	10.0833
Sample-II	6.5424
Sample-III	3.5583
Sample-IV	15.2726

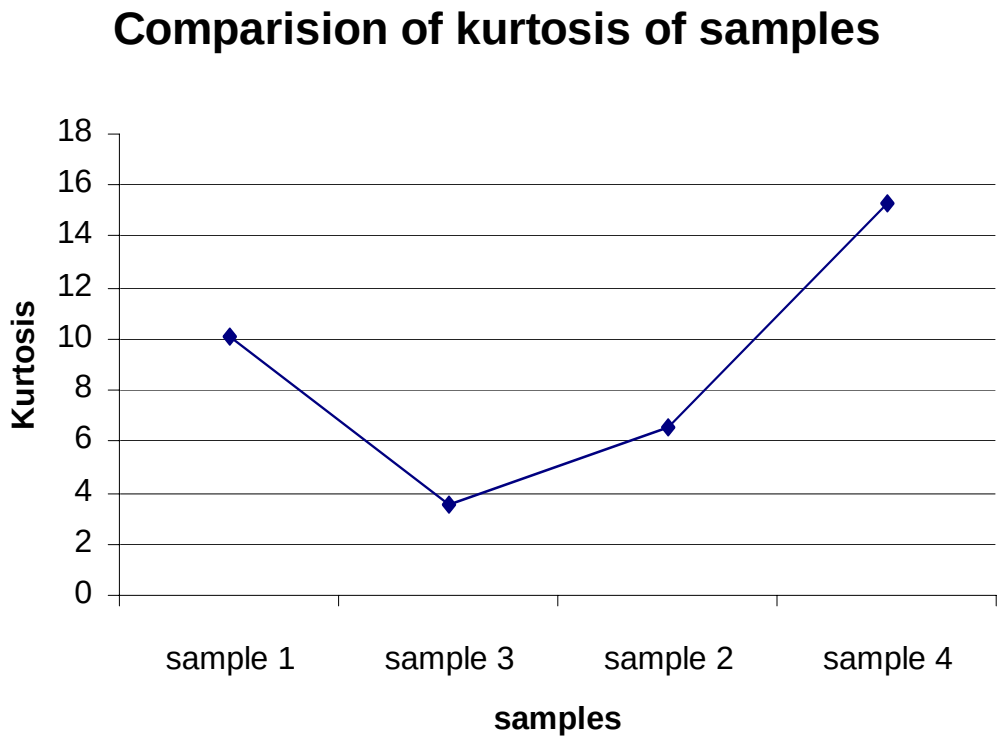

Fig. 33 Samples Vs Kurtosis Line graph.

Kurtosis higher than three predict higher contact and friction parameters with larger deviations compared to the Gaussian case, while distributions with kurtosis lower than three predict lower values than the Gaussian case. In the ca mse of a surface with kurtosis higher than three, the surface roughness is peaker. Therefore contact occurs first between two surfaces of kurtosis higher than three. Surfaces with kurtosis less than three will experience significant contact only when they are further approached to each other. Higher the value of kurtosis means more peak is the surface profile and more likely to wear fast than the surface profiles of less kurtosis value. From this graph though kurtosis value for sample II and III is less but due to third body abrasion the wear rate is high.

Variation of loss of weight due to wear test of the samples at constants speed of 60 r.p.m. , load = 10 N and time = 60 minutes.

Specimen	Weight loss (in gm)
Sample I	**0.0014**
Sample II	**0.0024**
Sample III	**0.0018**
Sample IV	**0.004**

Fig

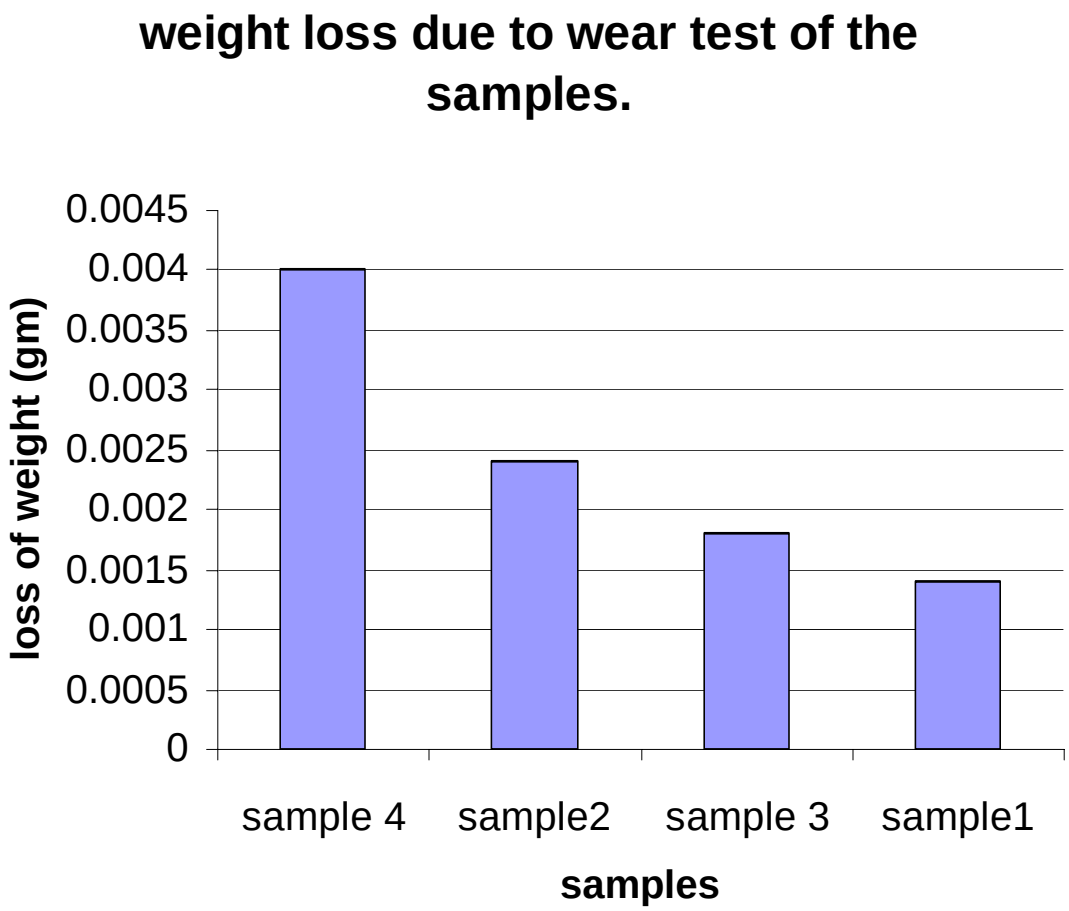

Fig.34 samples vs loss of weight due to wear test bar graph.

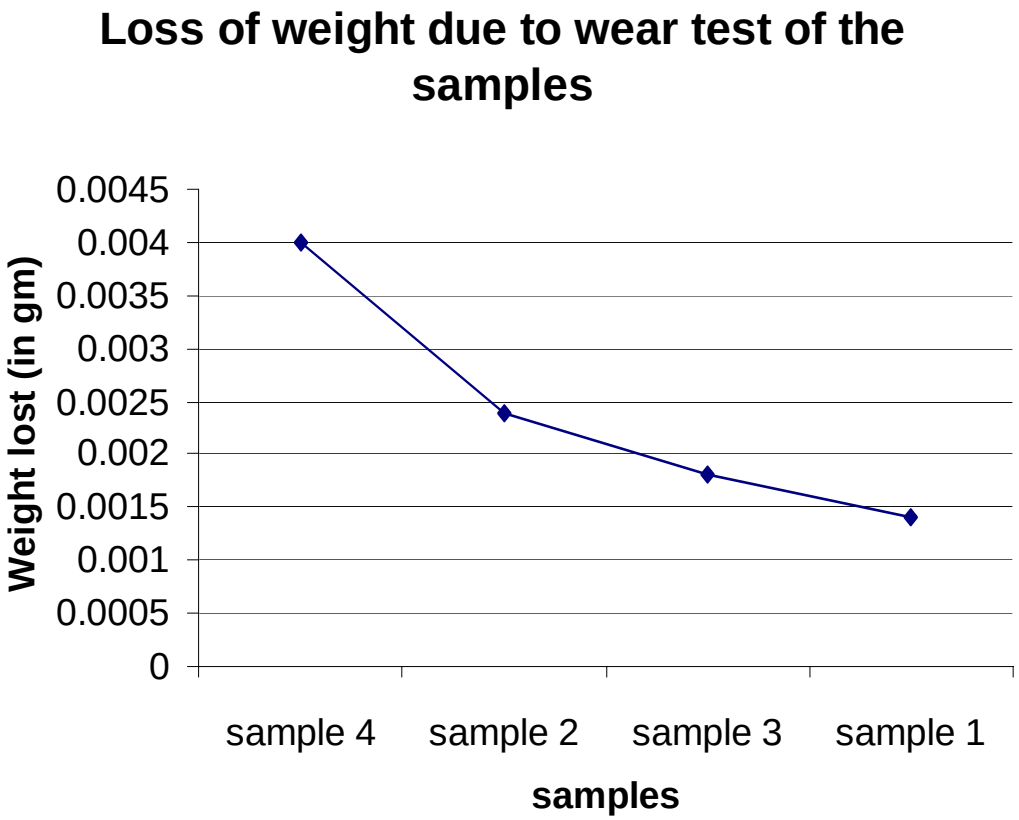

Fig. 35 Samples Vs Loss of weight due to wear test line graph

In this graph the weight loss due to friction for sample I is less than the others hence sample I has got better wear resistance property than the others. Hence sample I friction pad with four slots is more efficient than the other samples.

Comparison of percentage increase in life of samples tested at constant speed of 60 r.p.m. ,load = 10N and time = 60 minutes

Specimen	Percentage increase in life
Sample I	65
Sample II	40
Sample III	55
Sample IV	00

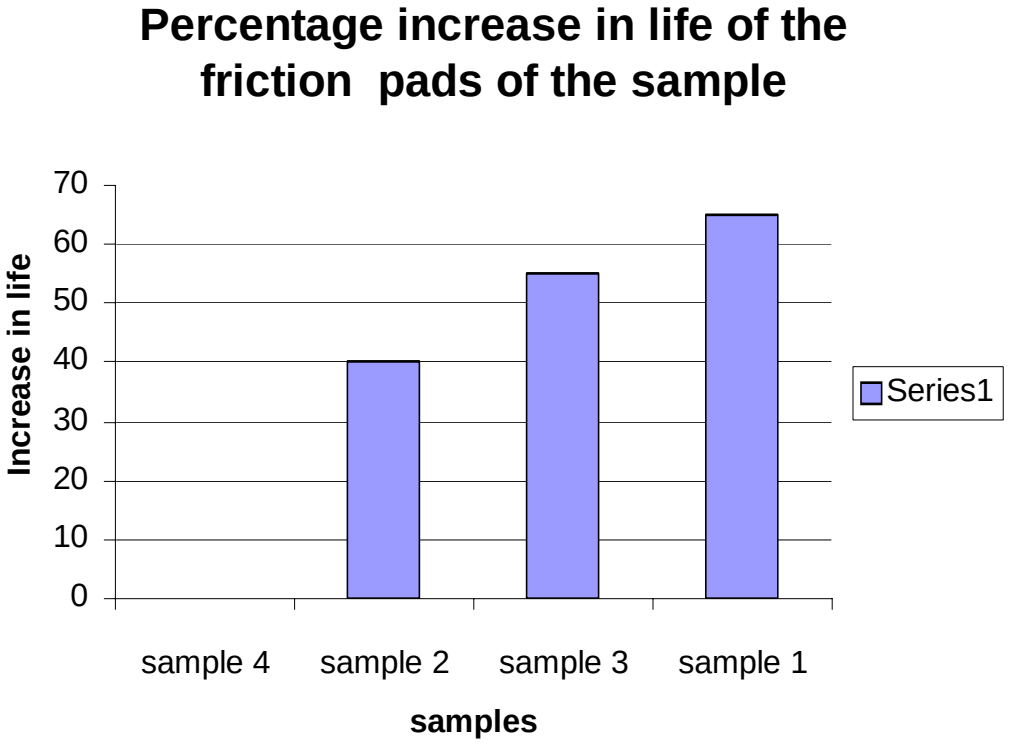

Fig. 36 Samples Vs Percentage increase in life bar graph

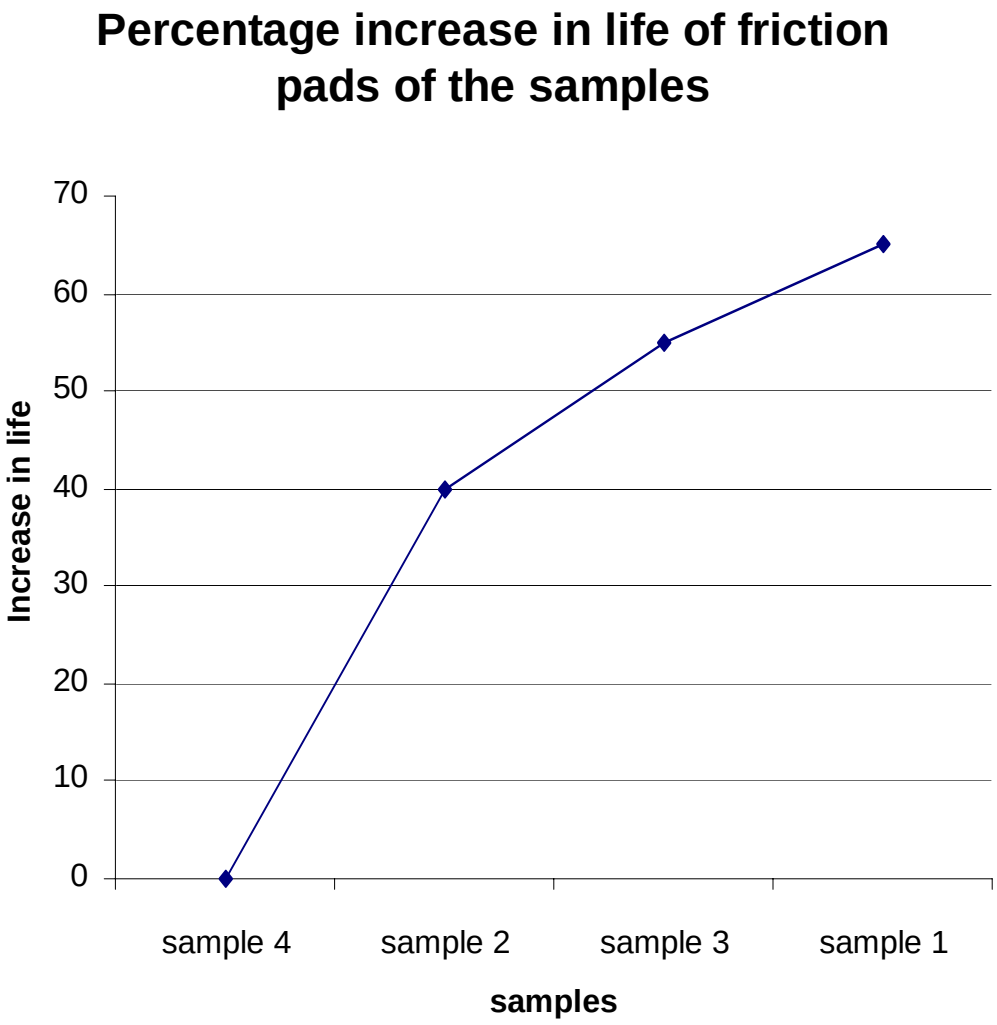

Fig.37 Samples Vs percentage increase in life of the samples line graph.

Analyzing the above two graphs shows that the sample with four slots has less wear rate than the others due to more cooling effect and less wear due to third body abrasion.

CHAPTER-7

CONCLUSIONS

From the investigation following conclusions were reached.

- Plastic deformation i.e. micro cutting and micro plugging was identified as the main wears mechanism operating on the worn surface of the ceramic materials.

- The mode and to some extent the amount of wear in ceramic material is very depend on the microstructure of the material.

- Sample-I friction pad with four radial slots had less wear rate as compared to others due to better cooling effect.

- As the friction pad slides over the rotor, ceramic particles are removed due to friction and they slide over the surface causing more removal of ceramic particles. But in case of friction pads with four slots, the free particle moves very less distance and falls in to the slots. Hence volume of material worn out due to third body abrasion is less.

- The interfacial temperature between the rotor and the friction pads will decrease, it leads to increase in efficiency of the rotors and friction pads.

- The efficiency of sample-I friction pad increased by 65%, hence that of the brake unit

- The overall down tine of the aircraft for replacement of brake unit will be less, as number of brake replacements will be less.

- As the operation and maintenance of an aircraft costs more, lot of manpower and material is saved due to increase in efficiency of the brake unit.

REFERENCES.

1. R. K. Pandey and O. P. Gandhi : Advances in Tribology and maintenance (2004)

2. Noureddine Tayebi, Andreas A Polycarpou: Modeling the effect of skewness and kurtosis on the static friction coefficient of rough surfaces. Tribology International (2004), Vol. 37, pp 491-505.

3. F. H. Stott: High temperature sliding wear of metals. Tribology International, (2002) Vol. 35 pp 489-495.

4. Yeau-Ren Jeng, Zhi-Way Lin, and Shiub-Hwa-Shyu: A microscopic wear measurement method for general surfaces. Tribology International, (2002) Vol. 124, pp 829-833.

5. Peter J Blau: (2001) Compositions, Functions and Testing of Friction Brake Materials and their Additives.

6. Taylor Habson: Talysurf Intra Operator Hand Book. (2001) pp 79-121.

7. Takahisa Kato, Hiroshi Soutome: Friction material design for brake pads using database. Tribology International (2001) Vol.44, pp 137-141.

8. Mikael Eriksson, Staffan Jacobson: Tribology surfaces of organic brake pads. Tribology International (2000) Vol. 33 pp 817-827.

9. K. H. Zum Gahr: Wear by hard particles. Tribology International (1998) Vol. 31 pp 587-596.

10. Yuji Hands, Takahisha Kato: Effects of Cu powder, BaSO4 and cashew dust on the wear and friction characteristics of automotive brake pads. Tribology International (1996) Vol. 39 pp 346-353.

11. Etsuo Marui, Masatoshi Hasimoto, Shinobu Kato, and Wataru Kojima: Dissipation of kinetic energy by slip at the interface of mating surfaces. Wear (1992) Vol.159 pp 141-150.

12. C. S. Ramesh, S. K. Seshadri and K. J. L. Iyer: A model for wear rates of composite coatings. Wear (1992) Vol. 156 pp 205-209.

13. O. O. Ajayi, K. C. Ludema: The effects of microstructure on wear modes of ceramic material. Wear (1992) Vol. 154 pp 371-385.

14. D. A, Rigney: Some thoughts on sliding wear. Wear (1992) Vol. 152 pp 187-192.

15. A. Fischer: Mechanism of high temperature sliding abrasion of metallic material. Wear (1992) Vol.152 pp 151-159.

16. K. H. Zum Gahr: Sliding wear of ceramic-ceramic, ceramic-steel steel-steel pairs in lubricated and unlubricated contact wear. Wear (1989) Vol. 133 pp 1-22.

17. A. W. Ruff: Comparison of standard test methods for non-lubricated sliding wear. Wear (1989) Vol. 134 pp 49-57.

18. G. W. Stachowiak, G. B. Stachowiak, A. W. Bachelor: Metallic film transfer during metal-ceramic unlubricated sliding. Wear (1989) Vol. 132 pp 361-381.

19. Joseph C Conway Jr., Robert N Pangborn, Paul H Cohel, Donald A Love : Dry sliding wear behaviour of an Si- Al-O-N ceramic. Wear (1988) Vol.126 pp 79-90.

20. Donald H Buckley, Kuzuhisha Miyoshi: Friction and wear of ceramics. Wear (1984) Vol. Pp 333-353.

21. A. G. M. Hunter and E. A. Smith: Measurement of surface roughness. Wear (1980) Vol. 59 pp 383-386.

22. S. K. Rakhee: Wear mechanism for asbestos-reinforced automotive friction materials. Wear (1974) Vol. 29 pp 391-393.

23. H. D. Bush, D. M. Rouson, S. E. Warren: The application of neutron activate analysis to the measurement of the wear of a friction materials. Wear (1972) Vol. 20 pp 221-225.

24. S. K. Rakhee: Wear of metal reinforced phenolic resin. Wear (1971) Vol. 18 pp 471-477.

25. A. E Anderson: Wear of brake materials. Wear control handbook ASME, pp 843-857.

26. A. E. Anderson: Friction and wear of automotive brakes. ASM hand book, Friction, Lubrication and wear technology. (1992) Vol. 18 pp 569-577.

27. L. Gudmand-Hoyer, A. Bach, G. T. Neilsen and Per Morgan: Tribological properties of automatic disc brakes with solid lubricants. Wear (1999) Vol. 232 pp 168-175.

28. G. J. Howell and A. Ball: Dry sliding wear of particulate reinforced aluminum alloys against automobile friction materials. Wear (1995) Vol. 181 pp 379-390.

29. D. Yadav and C.V.K. Singh, "Landing Response of Aircraft with Optimal Anti-skid
braking", Journal of Sound and Vibration, 181(3), 1995, pp 401-416.

30. G. Nicholson: "Facts About Friction", Gedoran Pub, Winchester, Virginia, 1995, pp.260.

31. http// www pdma. Com.: Some facts about sliding wear.

32. http// www ojps.aip/asme.com.

LIST OF FIGURES.

Fig.1 Landing gear system.
Fig.2 Main landing gear.
Fig.3 Main brake.
Fig.4 Cutaway view main brake assembly.
Fig.5 Brake unit exploded view.
Fig.6 Rotor and stator of brake unit.
Fig.7 Rotor and friction pads of aircraft brake unit.
Fig.8 Drawing for manufacturing disk and slider.
Fig.9 Manufactured sliding pin and separation of one segment of the rotor plate along with the friction plate.
Fig.10 Pin-On-Disk type test rig.
Fig.11 Manufactured sliding pins.
Fig.12 Rotor plate after removing one segment, Friction plates are placed above the plate.
Fig13. Sample-I Friction plate with four slots.
Fig.14 Sample-II Friction plate with two slots.
Fig.15 Sample-III friction plate with three slots.
Fig.16 Sample-IV Friction plate with plane sliding surface.
Fig.17 General surface texture (300× magnification) of sample before test.
Fig.18 Surface texture (300× magnification) of sample-I after test.
Fig.19 Surface texture (300×magnification) of sample-II after test.
Fig.20 Surface texture (300×magnification) of sample-III after test.
Fig.21 Surface texture (300×magnification) of sample-IV after test.
Fig.22 Samples Vs centerline average bar chart.
Fig.23 Samples Vs centerline average line chart.
Fig.24 Samples Vs root mean square bar chart.
Fig.25 Samples Vs root mean square line chart.
Fig.26 Samples Vs maximum height of the profile above the mean line of the surface within the sampling length bar graph.
Fig.27 Samples Vs maximum height of the profile above the mean line of the surface within the sampling length line graph.
Fig.28 Samples Vs maximum depth of the profile below the mean line of the surface within the sampling length bar graph.

Fig.29 Samples Vs maximum depth of the profile below the mean line of the surface within the sampling length line graph.
Fig.30 Samples Vs sum of the largest peak and largest valley of the profile within the sampling length bar graph.
Fig.31 Samples Vs sum of the largest peak and largest valley of the profile within the sampling length line graph.
Fig.32 Samples Vs skewness of the samples line graph.
Fig.33 Samples Vs kurtosis of the samples line graph.
Fig.34 Samples Vs loss of weight due to wear test of the samples bar graph.
Fig.35 Samples Vs loss of weight due to wear test of the samples line graph.
Fig.36 Samples Vs percentage increase in life of the friction pads of the samples bar graph.
Fig.37 Samples Vs percentage increase in life of the friction pads of the samples line graph.